The major and minor wall teichoic acids prevent the sidewall localization of vegetative DL-endopeptidase LytF in *Bacillus subtilis*

Hiroki Yamamoto,[1] Yukiko Miyake,[2] Miharu Hisaoka,[2] Shin-ichirou Kurosawa,[2] and Junichi Sekiguchi[2, 3]*

[1] *Experimental Farm and* [2] *Department of Applied Biology, Faculty of Textile Science and Technology, and* [3] *Division of Gene Research, Department of Life Sciences, Research Center for Human and Environmental Sciences, Shinshu University, 3-15-1 Tokida, Ueda-shi, Nagano 386-8567, Japan*

* Author for correspondence

E-mail: jsekigu@shinshu-u.ac.jp; Tel: (+81)-268-21-5344; Fax: (+81)-268-21-5345

Running title: Teichoic acid modification in the *B. subtilis* cell wall

Key words: cell separation enzyme, LysM motif, cell wall modification, teichoic acids, *Bacillus subtilis*

Summary

Cell separation in *Bacillus subtilis* depends on specific activities of DL-endopeptidases CwlS, LytF, and LytE. Immunofluorescence microscopy (IFM) indicated that the localization of LytF depended on its N-terminal LysM domain. In addition, we revealed that the LysM domain efficiently binds to PG prepared by chemically removing wall teichoic acids (WTAs) from the *B. subtilis* CW. Moreover, increasing amounts of the LysM domain bound to TagB- or TagO-depleted CWs. These results strongly suggested that the LysM domain specifically binds to PG, and that the binding may be prevented by WTAs. IFM with TagB-, TagF- or TagO-reduced cells indicated that LytF-6xFLAG was observed not only at cell separation site and poles but also as a helical pattern along the sidewall. Moreover, we found that LytF was localizable on the whole cell surface in TagB-, TagF-, or TagO-depleted cells. These results strongly suggest that WTAs inhibit the sidewall localization of LytF. Furthermore, the helical LytF localization was observed on the lateral cell surface in MreB-depleted cells, suggesting that cell wall modification by WTAs along the sidewall might be governed by an actin-like cytoskeleton homolog, MreB.

Introduction

The bacterial cell wall (CW) is mainly composed of mesh-like peptidoglycan (PG) and covalently linked anionic polymers such as wall teichoic acids (WTAs). PG is built from long glycan strands cross-linked by peptide side chains (Warth and Strominger, 1971; Foster and Popham, 2002). It was reported that CW assembly in *B. subtilis* occurred in both the cylindrical part of the wall and the septum (Clarke-Sturman *et al*., 1989; Mobley *et al*., 1984; Merad *et al*., 1989). Moreover, recent experiments involving fluorescent vancomycin (Van-FL) suggested that PG synthesis of the septum depends on divisome, whereas that of the sidewall occurs in a helical pattern governed by an actin-like homolog, Mbl (Daniel and Errington, 2003). Mbl forms a dynamic helical filament with other actin-like homologs, MreB and MreBH, beneath the cytoplasmic membrane along the sidewall (Jones *et al*., 2001; Carballido-López and Errington, 2003; Carballido-López *et al*., 2006). On the other hand, another approach involving Van-FL and ramoplanin, an antibiotic that specifically binds to the reducing end of the nascent glycan chain and lipid II, labeled with a fluorophore, BodipyFl, revealed that the side wall PG synthesis is governed in an Mbl-independent manner, since the helical pattern along the sidewall was observed even in an *mbl* null mutant (Tiyanont *et al*., 2006).

Anionic polymers, which are 35-60% of the vegetative cell wall, are mainly composed of major and minor WTAs under non-phosphate-limiting conditions (Foster and Popham, 2002). The major WTA-biosynthetic enzymes are encoded by *tagA*, *tagB*, *tagD*, *tagE*, *tagF*, *tagO*, *gtaB*, and *tagP* (*yvyH*) (Foster and Popham, 2002; Lazarevic *et al*., 2002). A recent report has demonstrated that six genes, the exceptions being *tagE* and *gtaB*, are essential in *B. subtilis* (Kobayashi *et al*., 2003). Moreover, an ABC transporter encoded by two essential

genes, *tagG* and *tagH*, is required for WTAs translocation and linkage to PG (Lazarevic and Karamata, 1995). Biosynthesis pathway of major WTA was essential but recently, D'Elia *et al*. (2006) reported that *tagO*, whose product catalyzes the first step in the WTA biosynthesis pathway, is dispensable for cell viability, and that a *tagO* null mutant shows slow growth, aberrant morphology and septation, and nonuniform PG thickness. In addition, they defined that *tagB*, *tagD*, and *tagF* are essential in the presence of *tagO*, but not in its absence. TagB and TagD are involved in the linkage unit synthesis of major and minor WTAs, and TagF is required for chain polymerization of the major WTA (Foster and Popham, 2002; Lazarevic *et al*., 2002). It remains to be resolved why only *tagO* is not essential and why the essential nature of other *tag* genes can be suppressed by the deletion in *tagO*. On the other hand, GtaB, an UDP-glucose pyrophosphorylase involved in the glucosylation of the major WTA, is not essential (Soldo *et al*., 1993; Varón *et al*., 1993). In addition, the biosynthesis pathway of minor WTA is not essential (Lazarevic *et al*., 2002; Freymond *et al*., 2006). The *ggaA* and *ggaB* genes are required for the biosynthesis of the galactosamine-containing minor WTA.

The cell separation event following septation is the final step of cell division in bacteria (Errington and Daniel, 2002). *B. subtilis* produces, at least, three DL-endopeptidases, CwlS (YojL) (Fukushima *et al*., 2006), LytE (CwlF) (Ishikawa *et al*., 1998; Margot *et al*., 1998), and LytF (CwlE) (Margot *et al*., 1999; Ohnishi *et al*., 1999), during vegetative growth. A triple mutant lacking these enzymes exhibited aggregated microfiber formation, indicating a cell separation defect (Fukushima *et al*., 2006). Among these vegetative DL-endopeptidases, LytF plays a major role in cell separation especially after the middle vegetative growth phase (Ohnishi *et al*., 1999; Yamamoto *et al*., 2003). The *lytF* gene is transcribed by $E\sigma^D$ RNA polymerase, and a *lytF* mutant shows a long chained cell morphology (Ohnishi *et al*., 1999) similar to that of a *sigD* mutant (Helmann *et al*., 1988). On the other hand, the *lytE* gene is

transcribed by $E\sigma^A$ and $E\sigma^H$ RNA polymerases, and a *lytE* mutant shows a slightly chained cell morphology, especially in the early vegetative growth phase (Ishikawa *et al*., 1998; Ohnishi *et al*., 1999). Carballido-López *et al*. (2006) have reported that a LytE-GFP fusion is localized not only at cell separation sites and poles but also along the sidewall under slight over-expression conditions. The former localization appears to be a septum dependent manner, and the latter one in an MreBH-dependent helical manner. MreBH is one of the actin-like homologs and plays an important role in cell morphogenesis by interacting with the C-terminal DL-endopeptidase domain of LytE (Carballido-López *et al*., 2006). In addition, *lytE* and *mreBH* mutants show similar CW-related defects under low Mg^{2+} conditions (Carballido-López *et al*., 2006). Moreover, Bisicchia *et al*. (2007) reported that the essential YycFG two-component system positively regulates the expression of two vegetative DL-endopeptidase genes, *lytE* and *cwlO* (*yvcE*). They revealed that a *lytE cwlO* double mutant strain is not viable and that cells depleted of CwlO and lacking LytE exhibit loss of lateral cell wall synthesis and cell elongation. Based on these findings, it is thought that LytE plays at least two roles; one is in cell separation at the septum, and the other in cell wall turnover along the sidewall. Recently, it was reported that the *cwlS* gene is expressed by $E\sigma^H$ RNA polymerase during the late vegetative and stationary phases (Britton *et al*., 2002), and that CwlS is the third vegetative DL-endopeptidase in *B. subtilis* (Fukushima *et al*., 2006). Subcellular localization analysis involving immunofluorescence microscopy (IFM) revealed that LytE, LytF and CwlO are potentially localized at cell separation sites and both poles (Yamamoto *et al*., 2003; Fukushima *et al*., 2006). Moreover, IFM and Western blot analysis revealed that the enzymes were degraded by CW-bound and extracellular proteases WprA and Epr, respectively, during the vegetative growth phase. The N-terminal domains of CwlS, LytE, and LytF include four, three, and five tandem repeats of the LysM motif, respectively,

which appears to be a general PG-binding module (Bateman and Bycroft, 2000; Buist *et al*., 2008), separated by serine-rich regions. Thus we presumed that the LysM domains of CwlS, LytE, and LytF play an important role in their specific localization at cell separation sites.

In this study, we have demonstrated that the N-terminal CW-binding domain of LytF is required for its specific localization at cell separation site and poles, and that the LysM motif in the domain is involved in the specific binding to naked PG not modified by WTAs. Moreover, the binding to the sidewall was mainly inhibited by anionic polymers, major and minor WTAs, in the vegetative CW.

Results

Localization of LytF depends on the N-terminal CW-binding domain

In this research, we used a LytF-6xFLAG fusion strain to obtain brighter foci than LytF-3xFLAG (Yamamoto *et al*., 2003) and also confirmed that the LytF-6xFLAG protein retains a cell separation activity as well as LytF (data not shown). We previously reported that the LytF-3xFLAG fusion protein is potentially localized at cell separation sites and cell poles after cell division in a *wprA epr* double mutant (Yamamoto *et al*., 2003). To determine whether this specific localization depends on the N-terminal CW-binding domain (CWB_E) or the C-terminal catalytic one (CTD_E) of LytF, we constructed two strains, YM1047 and YM1051, carrying *cwb_E*- and *ctd_E-6xflag* fusion genes at the *lytF* locus, respectively. Then we carried out IFM to detect the fusion proteins. IFM of the CWB_E-6xFLAG expressing cells clearly indicated that the fusion protein was localized at cell separation sites and poles (Fig. 1D, E and F). The localization pattern was very similar to that of LytF-6xFLAG (Fig. 1A, B and C). In addition, Western blot analysis indicated that LytF- and CWB_E-6xFLAGs were detected in the cell wall fraction (Fig. 2). On the other hand, we could not observe any CTD_E-6xFLAG foci on the cell surface (Fig. 1G, H and I). As supporting this result, Fig. 2 showed that CTD_E-6xFLAG was secreted in the culture medium but not localized on the cell wall. These results strongly suggest that the specific localization of LytF-6xFLAG depends on the N-terminal CWB_E domain including five direct repeats of the LysM motif. Moreover, to examine the septum localization of LytF in PBP 2B-depleted cells, we constructed a *pbpB*-conditional mutant, HY1054. For this purpose, we put the *pbpB* gene downstream of an IPTG-inducible promoter, P_{spac}. When IPTG was removed, cells began to elongate and

Fig. 1

Fig. 2

form filaments, and the septal localization of LytF was absent (*Supplementary material*, Fig. S1). The result suggests that septal PG synthesized by PBP 2B is required for the specific localization of LytF at cell separation sites, consistent with the LytE-GFP localization, as reported by Carballido-López *et al*. (2006).

GST-2xLysM protein specifically binds to PG in vitro

To further examine the CW-binding ability of the CWB_E and CTD_E domains, we constructed two expression plasmids, pGEX-2xLysM, carrying a glutathione-S-transferase (*gst*)-*2xlysM* fusion gene, and pGEXEtCTD, carrying a *gst-ctd*$_E$ (catalytic domain of LytF) fusion gene. We were able to purify the GST-2xLysM and GST-tECTD fusion proteins in a soluble fraction of *Escherichia coli* BL21 (pGEX-2xLysM or pGEXEtCTD) (data not shown). Though we also tried to purify the GST-1xLysM, -3xLysM, -4xLysM, and -5xLysM fusion proteins, we could not obtain them as soluble proteins because of their high insolubility (data not shown). Therefore the GST-2xLysM protein was used for the CW-binding assay *in vitro*. CW was prepared from *B. subtilis* 168 cells at the transition stage (OD_{600}~2.0) in LB medium, and PG was prepared by chemically removing WTAs from CW as described under Experimental procedures. We found that the intact GST protein (data not shown) and the GST-tECTD fusion protein (Fig. 3B) bound to neither CW nor PG under the assay conditions. The latter result clearly indicated that the C-terminal catalytic domain of LytF does not have the CW-binding activity, supporting the IFM observation of the CTD_E-6xFLAG localization (Fig. 1H and I). On the other hand, in the case of the GST-2xLysM fusion protein, small amount of the protein is able to bind to vegetative CW (Fig. 3A, lane P for CW). Moreover, large amount of the protein binds to PG (Fig. 3A, lane P

Fig. 3

for PG). This suggests that PG prepared by treatment with 10 % trichloroacetic acid (TCA) is a better substrate for the binding of the LysM domain than CW. Because the substances removed from CW on the TCA treatment are mainly anionic polymers such as WTAs (Pollack and Neuhaus, 1994), we inferred the PG-binding of the LysM domain might be prevented by WTAs.

CW-binding assay of the GST-2xLysM protein on CWs prepared from WTA mutants

WTAs of *B. subtilis* consist of major and minor forms, which differ in the repeating unit; the major WTA is a polymer of glycerol phosphate, whereas the minor form is made from *N*-acetylgalactosamine and glucose phosphate (Foster and Popham, 2002; Lazarevic *et al*., 2002). Both TagB and TagO are required for the linkage unit biosynthesis of major and minor WTAs (Foster and Popham, 2002; Lazarevic *et al*., 2002). Indeed, it has been reported that depletion of TagO caused a significant decrease in the CW phosphate content (Soldo *et al*., 2002; D'Elia *et al*. 2006). Since a binding assay has revealed that the PG-binding ability of the LysM domain appears to be prevented by anionic polymers among CW components, we examined the binding of the GST-2xLysM fusion protein to CWs prepared from TagB- and TagO-depleted cells (Fig. 3C). *In vitro* binding assay to CW prepared from TagB-depleted cells revealed a considerably increased amount of GST-2xLysM binding to CW (Fig. 3C, lane P for $TagB^-$). This appeared to exhibit that the ratio of unmodified PG is increased in the TagB-depleted CW, since the PG amounts of the $TagB^+$ and $TagB^-$ CWs are normalized in the assay conditions. In addition, a similar binding assay for CW from TagO-depleted cells indicated that TagO depletion gave rise to an increased amount of GST-2xLysM binding to CW (Fig. 3C, lane P for $TagO^-$). These findings strongly suggested

that the LysM motif in the CWB_E domain specifically recognizes and binds to PG, and that the binding is inhibited by CW modification with anionic polymers such as WTAs. Moreover, we found that considerable amount of GST-2xLysM bound to CW prepared from a *tagO* null mutant (Fig. 3D, lane P for Δ*tagO* CW) as compared to the wild-type CW (Fig. 3A, lane P for CW). Furthermore, a large amount of GST-2xLysM binding was observed in the Δ*tagO* PG prepared from the Δ*tagO* CW (Fig. 3D, lane P for Δ*tagO* PG). These results appeared to suggest that CW modification might not completely lack in the mutant, and that the unknown CW modification may be removable by 10% TCA treatment.

Helical localization of LytF on the lateral cell surface in WTA mutants affecting the linkage unit biosynthesis

To confirm the results of the CW-binding assay *in vitro*, we observed the LytF localization pattern in a *tagB*-conditional mutant. Since the *tagB* gene is essential and the product is involved in the linkage unit biosynthesis of major and minor WTAs (Soldo *et al*., 2002; D'Elia *et al*. 2006), here we used an IPTG-inducible conditional mutant, HY1058. When IPTG was reduced to 0.1 mM, the LytF-6xFLAG was seen not only at cell separation sites and poles but also on the lateral cell surface (83.7% of 92 cells) (Fig. 4C and D). Fig. 4 Interestingly, the latter signals formed a helical pattern in most cells (Fig. 4D and G, and *Supplementary material*, Fig. S2). Judging from the results of the *in vitro* CW-binding assay, we thought that the helical LytF cables along the sidewalls might correspond to the regions of naked PG not modified by WTAs. Moreover, TagB-depleted cells showed an aberrant morphology, and LytF was localized on almost the whole cell surface (100% of 50 cells) (without IPTG, Fig. 4E and F). In addition to the results for the *tagB*-conditional mutant, a

similar helix pattern and whole cell surface localization were seen in TagO-reduced (81.7% of 82 cells) (0.08 mM IPTG, Fig. 4J and K) and TagO-depleted (100% of 58 cells) (without IPTG, Fig. 4L and M) cells, respectively. TagO is also required for the first step of the linkage unit biosynthesis of major and minor WTAs (Soldo *et al*., 2002), but D'Elia *et al*. (2006) reported that the *tagO* gene was dispensable, and that a *tagO* null mutant showed slow growing phenotype and aberrant cell morphology. Thus we examined the LytF localization in a *tagO* null mutant (Fig. 4N and O). The result indicated that LytF is localizable on the whole cell surface as well as in the case of TagO-depleted cells. These observations strongly suggest that WTAs inhibit the LytF localization on the lateral cell surface.

LytF localization in WTA mutants affecting the main chain polymerization

In the previous section, we revealed that the linkage unit biosynthesis enzymes affect the sidewall localization of LytF. Next, we examined two main chain polymerization enzymes, TagF (Fig. 4P-U) for major WTA and GgaAB (Fig. 4V and W) for minor one. Since the *tagF* gene is essential and the product is involved in the main chain polymerization of major WTA (Pooley *et al*., 1992), here we used an IPTG-inducible conditional mutant, HY1059. We observed the helical pattern of LytF-6xFLAG in TagF-reduced cells (61.8% of 110 cells) (Fig. 4R and S) and the whole cell surface localization in TagF-depleted cells (100% of 60 cells) (Fig. 4T and U). Moreover, we performed IFM with a double null mutant of *ggaA* and *ggaB*, MH1036, which are involved in minor WTA synthesis (Freymond *et al*., 2006). As a result, we observed a weak helical pattern of LytF-6xFLAG along the sidewalls (46% of 50 cells) in the mutant strain (Fig. 4V and W). This helical pattern was very similar to those

observed in the TagB-, TagO- or TagF-reduced cells (Fig. 4D, K and S). However, whole cell surface localization of LytF was not observed in the *ggaAB* mutant (Fig. 4W), as compared to in the TagF-depleted cells (Fig. 4U). Taken together, these results strongly suggest that LytF is localizable in a helical manner on the cylindrical part of major WTA-reduced cells and minor WTA-lacking ones, and that major and minor WTAs are principal hindering components of LytF on the lateral cell surface.

WTA modification along the sidewalls is governed by an actin-like homolog, MreB

It is now clear that LytF forms a helical pattern along the sidewalls on the major WTA-reduced or minor WTA-lacking cell surface. Recent reports revealed that PG synthesis on the lateral cell surface occurs in a helical manner in *B. subtilis* (Daniel and Errington, 2003; Tiyanont *et al*., 2006). They supposed that the helical PG synthesis along the sidewalls might be governed by one of the actin-like homologs. Thus we examined whether or not actin-like homologs are involved in the modification of major and minor WTAs. For this purpose, we constructed three strains; one is a *mreBH* null mutant (MH1042), and the other two conditional mutants of *mbl* (HY1066) and *mreB* (HY1071). In the case of the *mreB* conditional mutant, an in-frame deletion (Δ*mreB*) was introduced at the *mreB* locus as described previously (Formstone and Errington, 2005). To observe the patterns of localization of LytF-6xFLAG in these mutants, we carried out IFM observation (Fig. 5). Fig. 5A-D showed that the *mreBH* null mutation did not affect the LytF localization, suggesting that MreBH is not involved in the WTA modification on the lateral CW. Moreover, Fig. 5E-H indicated that no significant difference of the LytF localization was observed in an *mbl*-conditional mutant strain with or without 12 mM xylose. Furthermore, we examined the

Fig. 5

effect of MreB-depletion on the LytF localization. Interestingly, Fig. 5K-N clearly showed that LytF-6xFLAG was localizable in a helical manner on the lateral cell surface in the MreB-reduced (80.6 % of 72 cells) and MreB-depleted cells (84.7% of 59 cells), this being very like the helical pattern observed in WTA-reduced cells (Fig. 4D, K and S). These results appeared to suggest that MreB depletion might affect the CW modification by WTAs. Moreover, the helical localization was seen in a *mreB* null mutant grown without Mg^{2+} (Fig. 5S and T) and in the presence of 2.5 mM $MgCl_2$ (Fig. 5Q and R), but not in the presence of 25 mM $MgCl_2$ (Fig. 5O and P). Formstone and Errington (2005) have reported that an in-frame *mreB* null mutant restored normal growth and morphology with the addition of 25 mM $MgCl_2$. Our results appeared to indicate that teichoic acid modification along the sidewall is also restored in the *mreB* null mutant by high Mg^{2+} supplementation. Taken together, these results strongly suggest that the CW modification along the sidewall might be governed by MreB.

Discussion

In this report, we revealed that the N-terminal putative CW-binding domain of the vegetative DL-endopeptidase, LytF, plays an important role in the specific localization to cell separation sites and poles (Figs. 1 and 2). In addition, a depletion experiment on an essential protein, PBP 2B, for septum formation demonstrated that septum biosynthesis is required for the LytF localization, suggesting that the N-terminal CW-binding domain of LytF binds to septal PG synthesized through the transpeptidase activity of PBP 2B (*Supplementary material*, Fig. S1). The CW-binding domain of LytF consists of five direct repeats of the LysM motif separated by serine-rich regions. The LysM motif has been reported to be a general PG-binding module (Bateman and Bycroft, 2000; Buist *et al*., 2008), and is conserved in some cell separation enzymes in bacteria, e.g. MurA of *Listeria monocytogenes* (Carroll *et al*., 2003), AcmA of *Lactococcus lactis* (Steen *et al*., 2003; Steen *et al*., 2005), and Sle1 of *Staphylococcus aureus* (Kajimura *et al*., 2005). Interestingly, it has been reported that a sensor protein having the LysM motif is also required for the recognition of symbiotic bacteria in plants (Madsen *et al*., 2003; Radutoiu *et al*., 2003). Thus, the LysM motif must be one of the targeting domains required for the septum localization of cell separation enzymes in bacteria. Indeed in *B. subtilis*, all three vegetative DL-endopeptidases, LytE, LytF, and CwlS, which are associated with cell separation, retain the LysM repeats in the N-terminal region (Yamamoto *et al*., 2003; Fukushima *et al*., 2006). In addition, we revealed that a GST-2xLysM fusion protein binds to PG prepared from vegetative CW *in vitro*, and that the binding is prevented by anionic polymers such as WTAs (Fig. 3A). Since it is thought that the LysM motif specifically binds to PG (Bateman and Bycroft, 2000; Buist *et al*., 2008; Steen *et al*., 2003; Steen *et al*., 2005), our results appear to be quite reasonable. These

observations have also been supported by the results of a similar binding assay involving CWs prepared from TagB- and TagO-depleted cells (Fig. 3C). TagB and TagO are required for the linkage unit biosynthesis of major and minor WTAs (Foster and Popham, 2002; Lazarevic *et al*., 2002; Soldo *et al*., 2002; D'Elia *et al*. 2006). Moreover, IFM for LytF-6xFLAG in either TagB-, TagO- or TagF-reduced cells showed that the fusion protein bound to lateral CW in a helical manner in addition to cell separation sites and poles (Fig. 4D, G, K and S, and *Supplementary material*, Fig. S2). Supporting our results, it has been reported that AcmA of *L. lactis* was localized at cell separation sites and that its localization was hindered by CW constituents (Steen *et al*., 2003; Steen *et al*., 2005). They have supposed that lipoteichoic acid is a candidate for hindering component. On the other hand, it is well known that WTAs such as teichoic and teichuronic acids are major components for CW modification in *B. subtilis* (Foster and Popham, 2002; Lazarevic *et al*., 2002). In addition, since Soldo *et al*. (1999) reported that the *tua* operon, which is involved in the teichuronic acid biosynthesis under phosphate-limiting conditions, was not transcribed during vegetative growth in LB medium, we inferred that the WTAs in the *B. subtilis* CW are the principal candidates for the inhibiting components of the LytF localization. Indeed, as compared with the wild-type CW, an increased amount of the GST-2xLysM protein bound to PG (Fig. 3A), which was chemically prepared from the wild-type CW by treatment with 10% trichloroacetic acid, and CWs prepared from either TagB- or TagO-depleted cells in which both major and minor WTAs would be reduced (Fig. 3C). Moreover, the binding assays involving CW and PG prepared from a *tagO* null mutant strain appeared to suggest that unknown CW modification might still remain in the mutant cells (Fig. 3D). This unknown CW modification may suppress the lethality of the *tagO* null mutation.

Among *B. subtilis* WTAs, the major WTA is a very important component of the *B. subtilis*

cell wall since its deficiency affects cell morphology (D'Elia *et al*. 2006), whereas the minor WTA is not (Estrela *et al*., 1991; Freymond et al., 2006). However, it has been unclear how and where CW modification occurs. Our IFM observation results for some WTA-related mutants provided us with several important clues relating to the mode of CW modification with major and minor WTAs. In TagB- or TagO-reduced cells, LytF is localized not only at cell separation sites and poles but also in a helical manner along the sidewall (Fig. 4D, G and K, and *Supplementary material*, Fig. S2). Moreover, whole cell surface localization of LytF was observed in TagB- or TagO-depleted cells in which the linkage unit biosynthesis of major and minor WTAs would be abolished (Fig. 4F and 4M). Furthermore, LytF cables were readily observed in TagF-reduced cells in which the main chain polymerization of major WTA would be affected (Fig. 4S). In addition, helical LytF localization was observed in a double null mutant of *ggaA* and *ggaB* in which the main chain synthesis of minor WTA would be abolished (Fig. 4W), but whole cell surface localization seen in TagB-, TagO-, and TagF-depleted cells (Fig. 4F, M and U) was not observed in the *ggaAB* null mutant ones (Fig. 4W). These results suggest that major WTA is a main hindering component for the LytF localization on the cylindrical part of the rod-shaped cell. Based on the findings of the *in vitro* CW-binding assay, it was thought that CW modification by WTAs might be poor in the LytF-binding regions. Thus there is a possibility that WTA modification might be reduced at the septum rather than in the sidewall. On the other hand, Formstone *et al*. (2008) reported that WTA synthesis enzymes localized not only along the sidewall but also to the cell division sites, suggesting that WTA modification might not be reduced at the septum. To answer this discrepancy, the exact nature of septum localization of LytF is currently under study.

In this study, we found that helical LytF localization was observed in several WTAs

mutants (Fig. 4D, G, K and S, and *Supplementary material*, Fig. S2). These results appeared to suggest, at least, two possibilities. One is that WTA modification and nascent PG incorporation are simultaneously occurred in a helical manner along the sidewall, and the other is that PG synthesis is occurred in a helical manner but WTA modification is not. As supporting the former possibility, Formstone *et al*. (2008) revealed that teichoic acid synthetic enzymes (TagB/F/G/H/O) form a large multi-enzyme complex and localize in a helical pattern.

Carballido-López *et al*. (2006) demonstrated that MreBH appears to form a filamentous and helical structure complex with other actin-like homologs, MreB and Mbl, just beneath the cytoplasmic membrane. In addition to this complex formation by three MreBs, MreBH controls the lateral cell surface localization of DL-endopeptidase LytE by means of a physiological interaction, and this interaction is especially required for survival at low Mg^{2+} concentrations (Carballido-López *et al*., 2006). The authors inferred that MreBH and LytE might play roles in the helical pattern insertion of both PG-synthesizing and PG-hydrolyzing activities. Thus, we examined whether or not the CW modification by WTAs might be governed by helical scaffolds, e.g. an actin-like homolog, Mbl, MreB, or MreBH, just beneath the cytoplasmic membrane. Our results suggested that MreBH and Mbl did not affect the LytF localization (Fig. 5D and H), suggesting that these two actin-like homologs might not be involved in the WTA modification. On the other hand, our IFM observations indicated that the helical LytF localization was observed only on the cell surface in both MreB-reduced and MreB-depleted cells (Fig. 5L and N). This helical pattern was very like that observed in the WTAs mutants (Fig. 4D, G, K and S), strongly suggesting that an actin-like filament, MreB, might govern CW modification by major and minor WTAs. However, whole cell surface localization of LytF was not observed in MreB-depleted cells

(Fig. 5N) as compared with in TagB-, TagO-, or TagF-depleted cells (Fig. 4F, M and U). We presume that regular and helical CW modification by WTAs may be abolished, but the irregular modification continued in MreB-depleted cells because the substrates of WTAs were supplied. On the other hand, they were not supplied in TagB-, TagO-, or TagF-depleted cells. Thus, whole cell surface localization of LytF may be observed (Fig. 4F, M and U). Moreover, since helical LytF cable appeared to be seen in the nascent PG region, helical PG synthesis might occur in MreB-depleted cells as well as in the WTAs mutants. Formstone and Errington (2005) revealed that a *mreB* null mutant restores the normal growth and cell morphology in the presence of high concentrations of Mg^{2+}, and that MreB is not required for cylindrical PG synthesis and chromosome segregation in the presence of SMM (sucrose, maleic acid, and $MgCl_2$). Thus we examined whether the helical LytF localization changes in the presence of high concentrations of Mg^{2+}. The result clearly indicated that the helical LytF localization in a *mreB* null mutant is lost in the presence of the 25 mM $MgCl_2$ (Fig. 5P), suggesting that CW modification was restored in the *mreB* null mutant under high Mg^{2+} concentrations. This result appeared to support a very recent finding that a *mreB* disruption did not affect the helical localization of Tag proteins with the addition of sucrose, maleic acid and Mg^{2+} (Formstone *et al*., 2008). Taken together, these results suggest that CW modification by WTAs along the sidewall might be governed by an actin-like cytoskeleton homolog, MreB, in a helical manner. It appears to be quite reasonable if CW modification is carried out in a helical manner as well as PG synthesis and PG hydrolysis. Further experiments are needed to demonstrate whether or not CW modification occurs in a helical manner, and to determine that what mechanism and factors lie between a bacterial actin-like homolog, MreB, and CW modification by WTAs.

Experimental procedures

Bacterial strains and plasmids

The strains of *B. subtilis* and *E. coli*, and plasmids used in this study are listed in Table 1. *B. subtilis* WEC, a double mutant strain of *wprA* and *epr* without any antibiotic resistance genes, was used as the parent strain throughout this study.

General methods

B. subtilis strains were grown in Luria-Bertani (LB) medium (Sambrook *et al*., 1989) at 37˚C unless otherwise noted. When necessary, chloramphenicol, kanamycin, spectinomycin, and erythromycin were added to final concentrations of 5, 5, 100, and 0.3 μg ml^{-1}, respectively. To culture conditional mutant strains of *pbpB*, *tagB*, *tagF*, and *tagO*, isopropyl-β-D-thiogalactopyranoside (IPTG) was added to final concentrations of 0.4, 0.8, 0.4, and 0.4, respectively. To pre-culture xylose-inducible *mbl* and *mreB* mutants, 12 and 2 mM xylose, respectively, at final concentrations was added to LB medium. *E. coli* strains were cultured in LB medium at 37˚C. If necessary, ampicillin was added to a final concentration of 100 μg ml^{-1}.

DNA manipulations and *E. coli* transformation were performed by standard methods (Sambrook *et al*., 1989). *B. subtilis* transformation was performed by the conventional transformation procedure (Anagnostopoulos and Spizizen, 1961).

Sample preparation for IFM observation

For IFM observation, cells from an overnight culture at 25˚C in LB medium were twenty-fold diluted in 5 ml of fresh LB medium. Then the cells were grown to the exponential phase at 37˚C. A culture exhibiting an optical density at 600 nm (OD_{600}) of 0.25 was centrifuged, and the cells were suspended in 5 ml of fresh LB medium. In the case of conditional mutants of *pbpB*, *tagB*, *tagF*, and *tagO*, the cells were suspended in 5 ml of fresh LB medium with or without IPTG. For a xylose-inducible mutant of *mbl* (P_{xyl}-*mbl*) and *mreB* (P_{xyl}-*mreB*), 12 and 2 mM xylose, respectively, was added to the medium instead of IPTG. These cultures were allowed to grow until OD_{600} reached ~1.8. Cells corresponding to 0.5 of an OD_{600} unit were harvested and fixed. Sample preparation for IFM observation was carried out as described previously (Yamamoto *et al*., 2003) with a minor modification, as follows. For the detection of anti-FLAG antibody with Cy3, a sheep anti-mouse IgG Cy3 conjugate antibody (Sigma) was used at 1:800 dilution.

Fluorescence microscopy

Fluorescence microscopy was performed as described previously (Yamamoto *et al*., 2003) with an Olympus BX61 microscope equipped with a BX-UCB control unit, a UPPlan Apo Fluorite phase-contrast objective (magnification, X100; numerical aperture, 1.3), and standard filter sets for visualizing DAPI, FITC and rhodamine (for Cy3). The exposure times were 0.1 s for phase-contrast microscopy, 0.1 s (gain 2) for Cy3. Cells were photographed with a charge-coupled device camera (CoolSNAP HQ; Nippon Roper) driven by Metamorph software (version 4.6; Universal Imaging). For Cy3 imaging out of focus light was removed

using the 2D Deconvolution utility of AutoDeblur software. All images were processed with Adobe Photoshop software. For z axis imaging, fluorescence microscopy was performed with an AxioImager M1 microscope, a Plan-APOCHROMAT Fluorite differential interference objective (magnification, X63; numerical aperture, 1.4), and standard filter sets for visualizing rhodamine (for Cy3). The exposure times were 0.1 s for phase-contrast microscopy, 0.1 s (gain 1) for Cy3. Cells were photographed with a charge-coupled device camera (AxioCam MRm; Carl Zeiss) driven by AxioVision software (version 4.6; Carl Zeiss). The 3D Deconvolution utility of AxioVision software was used for z-axis imaging. All images were processed with AxioVision and Adobe Photoshop software.

Preparation of cell wall (CW), peptidoglycan (PG) and cell surface proteins

CW of the *B. subtilis* strain was prepared essentially as described previously (Fein and Rogers, 1976; Kuroda and Sekiguchi, 1990). Moreover, for preparation of purified PG, the CW was treated twice in 10% trichloroacetic acid (TCA) at 37 °C for 1 day to remove acid labile components such as WTAs and polysaccharide (DeHart *et al*., 1995). The amount of PG was calculated by measuring the OD_{540} value. One OD_{540} (ml^{-1}) unit is equivalent to 6.45 mg ml^{-1} of PG. For preparation of cell surface proteins, we used an extraction method involving high concentrations of LiCl described previously (Rashid *et al*., 1995). For concentration of proteins secreted in the culture medium, TCA precipitation (final concentration 2%) was used as described previously (Rashid *et al*., 1995).

Overexpression and purification of the GST-2xLysM and GST-tECTD fusion proteins

E. coli BL21(pGX-2xLysM or pGXEtCTD) was cultured in 400 ml of LB medium containing 100 μg/ml of ampicillin until an OD_{600} of approximately 1.5 at 37°C. Then IPTG was added to the culture to the final concentration of 1 mM, followed by further incubation for 0.5 h. The culture was then centrifuged, and the pellet was suspended in 10 ml of ice-cold PBST buffer (80 mM NaH_2PO_4, 20 mM Na_2HPO_4, 100 mM NaCl [pH 7.5], and 1% Tween 20). After ultrasonication (Sonics and Materials) on ice, the suspension was centrifuged, and the supernatant was filtered through a 0.45 μm-pore-size membrane filter (Nalgene), followed by application to a GSTrap column (1 ml; GE Healthcare). The column was washed with 20 ml of ice-cold PBST buffer, and then the GST-2xLysM or GST-tECTD protein was eluted with 5 ml of elution buffer (50 mM Tris-HCl [pH 8.0], 10 mM reduced glutathione, 1% Tween 20). The eluate was dialysed twice against 500 ml of PBS buffer at 4˚C for more than 3 h.

SDS-PAGE and Western blot analysis

Sodium dodecyl sulfate-polyacrylamide gel electrophoresis (SDS-PAGE) of proteins was performed in 12% (wt/vol) polyacrylamide gels as described by Laemmli (1970). For sample preparation, an equal volume of 2x SDS-PAGE sample buffer (Laemmli, 1970) was added to a protein solution. After staining the gel, a Lane and Spot Analyzer (Atto) was used to calculate the amount of protein in a band according to the manufacturer's instructions. Western blot analysis for the FLAG-fusion proteins was performed as described previously (Yamamoto *et al*., 2003).

In vitro *binding assay to CW or PG*

The CW-binding assay with the GST-2xLysM or GST-tECTD protein was examined in 60 µl of PBST buffer containing 20 µg of the purified protein, and CW or PG corresponding to 75 µg of PG. For the CW-binding assay to CWs prepared from TagB- or TagO-depleted cells, the CW amounts were normalized as to the PG amount as follows. A part of the TagB- or TagO-depleted CWs was treated twice in 10% TCA at 37 °C for 1 day to remove WTAs, and then the PG amount was calculated by measuring the OD_{540} value. Finally, the TagB- or TagO-depleted CWs including 75 µg of PG was added to a 60 µl of the reaction mixture. After 15-min incubation on ice, the reaction mixture was centrifuged. Then the supernatant, as the non-binding fraction, was transferred to a new tube and an equal volume of 2x SDS-PAGE sample buffer (Laemmli, 1970) was added. The pellet, as the CW- or PG-binding fraction, was washed once with 60 µl of PBST buffer, and then 120 µl of 1x SDS-PAGE sample buffer was added to the pellet. After boiling for 5 min, samples were applied to an SDS-PAGE gel.

Acknowledgements

We would like to thank Dr T. Msadek and Dr M. Débarbouillé for kindly providing plasmids pXT and pMAD. We thank the members of our group for the helpful discussions and advice. We also thank Mr. S. Ooiwa, Ms. N. Hariyama, and Mr. T. Sakamoto for their technical assistance. This work was supported by Grants-in-Aid for Scientific Research (B) (19380047) and by the New Energy and Industrial Technology Department Organization (NEDO) to J.S., for Scientific Research (C) (19580085) to H.Y., and for the Global COE programs (to J.S. and H.Y.) of the Ministry of Education, Culture, Sports, Science, and

Technology of Japan.

Supplementary material

Plasmid construction

Construction of mutants and FLAG fusion strains

Table S1. Primers used in this study.

Figure S1. LytF-6xFLAG localization in PBP 2B-depleted cells.

Figure S2. A z-stack image of LytF-6xFLAG localization in a TagB-reduced cell.

References

Anagnostopoulos, C., and Spizizen, J. (1961) Requirements for transformation in *Bacillus subtilis*. *J Bacteriol* **81**: 741-746.

Arnaud, M., Chastanet, A., and Débarbouillé, M. (2004) New vector for efficient allelic replacement in naturally nontransformable, low-GC-content, Gram-positive bacteria. *Appl Environ Microbiol* **70**: 6887-6891.

Bateman, A., and Bycroft, M. (2000) The structure of a LysM domain from *E. coli* membrane-bound lytic murein transglycosylase D (MltD). *J Mol Biol* **299**: 1113-1119.

Bisicchia, P., Noone, D., Lioliou, E., Howell, A., Quigley, S., Jensen, T., Jarmer, H., and Devine, K.M. (2007) The essential YycFG two-component system controls cell wall metabolism in *Bacillus subtilis*. *Mol Microbiol* **65**: 180-200.

Britton, R.A., Eichenberger, P., Gonzalez-Pastor, J.E., Fawcett, P., Monson, R., Losick, R., and Grossman, A.D. (2002) Genome-wide analysis of the stationary-phase sigma factor (sigma-H) regulon of *Bacillus subtilis*. *J Bacteriol* **184**: 4881-4890.

Buist, G., Steen, A., Kok, J., and Kuipers, O.P. (2008) LysM, a widely distributed protein motif for binding to (peptido)glycans. *Mol Microbiol* **68**: 838-847.

Carballido-López, R., and Errington, J. (2003) The bacterial cytoskeleton. *In vivo* dynamics of the actin-like protein Mbl of *Bacillus subtilis*. *Dev Cell* **4**: 19-28.

Carballido-López, R., Formstone, A., Li, Y., Ehrlich, S.D., Noirot, P., and Errington, J. (2006) Actin homolog MreBH governs cell morphogenesis by localization of the cell wall hydrolase LytE. *Dev Cell* **11**: 399-409.

Carroll, S.A., Hain, T., Technow, U. Darji, A., Pashalidis, P., Joseph, S.W., and Chakraborty, T. (2003) Identification and characterization of a peptidoglycan hydrolase, MurA, of

Listeria monocytogenes, a muramidase needed for cell separation. *J Bacteriol* **185**: 6801-6808.

Clarke-Sturman, A.J., Archibald, A.R., Hancock, I.C., Harwood, C.R., Merad, T., and Hobot, J.A. (1989) Cell wall assembly in *Bacillus subtilis*: partial conservation of polar wall material and effect of growth conditions on the pattern of incorporation of new material at the polar caps. *J Gen Microbiol* **135**: 657-665.

Daniel, R.A., and Errington, J. (2003) Control of cell morphogenesis in bacteria: two distinct ways to make a rod-shaped cell. *Cell* **113**: 767-776.

DeHart, H.P., Heath, H.E., Heath, L.S., LeBlanc, P.A., and Sloan, G.L. (1995) The lysostaphin endopeptidase resistance gene (*epr*) specifies modification of peptidoglycan cross bridges in *Staphylococcus simulans* and *Staphylococcus aureus*. *Appl Environ Microbiol* **61**: 1475-1479.

D'Elia, M.A., Millar, K.E., Beveridge, T.J., and Brown, E.D. (2006) Wall teichoic acid polymers are dispensable for cell viability in *Bacillus subtilis*. *J Bacteriol* **188**: 8313-8316.

Derré, I., Rapoport, G., and Msadek, T. (2000) The CtsR regulator of stress response is active as a dimmer and specifically degraded *in vivo* at 37˚C. *Mol Microbiol* **38**: 335-347.

Errington, J., and Daniel, R.A. (2002) Cell division during growth and sporulation. In *Bacillus subtilis and Its Closest Relatives: from Genes to Cells.* Sonenshein, A.L., Losick, and R., Hoch, J.A. (eds.). Washington, DC: American Society for Microbiology Press, pp. 97-109.

Estrela, A.I., Pooley, H.M., de Lencastre, H., and Karamata, D. (1991) Genetic and biochemical characterization of *Bacillus subtilis* 168 mutants specifically blocked in the synthesis of the teichoic acid poly(3-*O*-ß-D-glucopyranosyl-*N*-acetylgalactosamine

1-phospate): *gneA*, a new locus, is associated with UDP-*N*-acetylglucosamine 4-epimerase activity. *J Gen Microbiol* **137**: 943-950.

Fein, J.E., and Rogers, H.J. (1976) Autolytic enzyme-deficient mutants of *Bacillus subtilis* 168. *J Bacteriol* **127**: 1427-1442.

Formstone, A., and Errington, J. (2005) A magnesium-dependent *mreB* null mutant: implications for the role of *mreB* in *Bacillus subtilis*. *Mol Microbiol* **55**: 1646-1657.

Formstone, A., Carballido-López, R., Noirot, P., Errington, J., and Scheffers, D.J. (2008) Localization and interactions of teichoic acid synthetic enzymes in *Bacillus subtilis*. *J Bacteriol* **190**: 1812-1821.

Foster, S.J., and Popham, D.L. (2002) Structure and synthesis of cell wall, spore cortex, teichoic acids, S-layers, and capsules. In *Bacillus subtilis and Its Closest Relatives: from Genes to Cells*. Sonenshein, A.L., Losick, R., and Hoch, J.A. (eds). Washington, DC: American Society for Microbiology Press, pp. 21-41.

Freymond, P., Lazarevic, V., Soldo, B., and Karamata, D. (2006) Poly(glucosyl-*N*-acetylgalactosamine 1-phosphate), a wall teichoic acid of *Bacillus subtilis* 168: its biosynthetic pathway and mode of attachment to peptidoglycan. *Microbiology* **152**: 1709-1718.

Fukushima, T., Afkham A., Kurosawa, S., Tanabe, T., Yamamoto, H., and Sekiguchi, J. (2006) A new D,L-endopeptidase gene product, YojL (renamed CwlS), plays a role in cell separation with LytE and LytF in *Bacillus subtilis*. *J Bacteriol* **188**: 5541-5550.

Helmann, J.D., Marquez, L.M., and Chamberlin, M.J. (1988) Cloning, sequencing, and disruption of the *Bacillus subtilis* sigma 28 gene. *J Bacteriol* **170**: 1568-1574.

Ishikawa, S., Hara, Y., Ohnishi, R., and Sekiguchi, J. (1998) Regulation of a new cell wall hydrolase gene, *cwlF*, which affects cell separation in *Bacillus subtilis*. *J Bacteriol* **180**:

2549-2555.

Jones, L.J., Carballido-López, R., and Errington, J. (2001) Control of cell shape in bacteria: helical, actin-like filaments in *Bacillus subtilis*. *Cell* **104**: 913-922.

Kajimura, J., Fujiwara, T., Yamada, S., Suzawa, Y., Nishida, T., Oyamada, Y., Hayashi, I., Yamagishi, J., Komatsuzawa, H., and Sugai, M. (2005) Identification and molecular characterization of an *N*-acetylmuramoyl-L-alanine amidase Sle1 involved in cell separation of *Staphylococcus aureus*. *Mol Microbiol* **58**: 1087-1101.

Kobayashi, K., Ehrlich, S.D., Albertini, A., Amati, G., Andersen, K.K., Arnaud, M., *et al.* (2003) Essential *Bacillus subtilis* genes. *Proc Natl Acad Sci USA* **100,** 4678-4683.

Kuroda, A., and Sekiguchi, J. (1990) Cloning, sequencing and genetic mapping of a *Bacillus subtilis* cell wall hydrolase gene. *J Gen Microbiol* **136**: 2209-2216.

Laemmli, U.K. (1970) Cleavage of structural proteins during the assembly of the head of bacteriophage T4. *Nature* **227**: 680-685.

Lazarevic, V., and Karamata, D. (1995) The *tagGH* operon of *Bacillus subtilis* 168 encodes a two-component ABC transporter involved in the metabolism of two wall teichoic acids. *Mol Microbiol* **16**: 345-355.

Lazarevic, V., Pooley, H.M., Mauël, C., and Karamata, D. (2002) Teichoic and teichuronic acids from Gram-positive bacteria. In *Biopolymers, Vol. 5, Polysaccharides I: Polysaccharides from Prokaryotes*. Vandamme, E.J., de Baets, S., and Steinbüchel, A. (eds). Weinheim: Wiley-VCH. pp. 465-492.

Margot, P., Pagni, M., and Karamata, D. (1999) *Bacillus subtilis* 168 gene *lytF* encodes a γ-D-glutamate-*meso*-diaminopimelate muropeptidase expressed by the alternative vegetative sigma factor, σ^D. *Microbiology* **145**: 57-65.

Margot, P., Wahlen, M., Gholamhuseinian, A., Piggot, P., and Karamata, D. (1998) The *lytE*

gene of *Bacillus subtilis* 168 encodes a cell wall hydrolase. *J Bacteriol* **180**: 749-752.

Madsen, E.B., Madsen, L.H., Radutoiu, S., Olbryt, M., Rakwalska, M., Szczyglowski, K., Sato, S., Kaneko, T., Tabata, S., Sandal, N., and Stougaard, J. (2003) A receptor kinase gene of the LysM type is involved in legume perception of rhizobial signals. *Nature* **425**: 637-640.

Merad, T., Archibald, A.R., Hancock, I.C., Harwood, C.R., and Hobot, J.A. (1989) Cell wall assembly in *Bacillus subtilis*: visualization of old and new wall material by electron microscopic examination of samples stained selectively for teichoic acid and teichuronic acid. *J Gen Microbiol* **135**: 645-655.

Mobley, H.L., Koch, A.L., Doyle, R.J., and Streips, U.N. (1984) Insertion and fate of cell wall in *Bacillus subtilis*. *J Bacteriol* **158**: 169-179.

Ohnishi, R., Ishikawa, S., and Sekiguchi, J. (1999) Peptidoglycan hydrolase LytF plays a role in cell separation with LytE during vegetative growth of *Bacillus subtilis*. *J Bacteriol* **181**: 3178-3184.

Pollack, J.H., and Neuhaus, F.C. (1994) Changes in wall teichoic acid during the rod-sphere transition of *Bacillus subtilis* 168. *J Bacteriol* **176**: 7252-7259.

Pooley, H.M., Abellan, F.X., and Karamata, D. (1992) CDP-glycerol: poly (glycerophosphate) glycerophosphotransferase, which is involved in the synthesis of the major wall teichoic acid in *Bacillus subtilis* 168, is encoded by *tagF* (*rodC*). *J Bacteriol* **174**: 646-649.

Radutoiu, S., Madsen, L.H., Madsen, E.B., Felle, H.H., Umehara, Y., Gronlund, M., Sato, S., Nakamura, Y., Tabata, S., Sandal, N., and Stougaard, J. (2003) Plant recognition of symbiotic bacteria requires two LysM receptor-like kinases. *Nature* **425**: 585-592.

Rashid, M.H., Sato, N., and Sekiguchi, J. (1995) Analysis of the minor autolysins of *Bacillus*

subtilis during vegetative growth by zymography. *FEMS Microbiol Lett* **132**: 131-137.

Sambrook, J., Fritsch, E.F., and Maniatis, T. (1989) *Molecular Cloning*: *A Laboratory Manual*. Cold Spring Harbor, NY: Cold Spring Harbor Laboratory Press.

Soldo, B., Lazarevic, V., and Karamata, D. (2002) *tagO* is involved in the synthesis of all anionic cell-wall polymers in *Bacillus subtilis* 168. *Microbiology* **148**: 2079-2087.

Soldo, B., Lazarevic, V., Margot, P., and Karamata, D. (1993) Sequencing and analysis of the divergon comprising *gtaB*, the structural gene of UDP-glucose pyrophosphorylase of *Bacillus subtilis* 168. *J Gen Microbiol* **139**: 3185-3195.

Soldo, B., Lazarevic, V., Pagni, M., and Karamata, D. (1999) Teichuronic acid operon of *Bacillus subtilis* 168. *Mol Microbiol* **31**: 795-805.

Steen, A., Buist, G., Horsburgh, G.J., Venema, G., Kuipers, O.P., Foster, S.J., and Kok, J. (2005) AcmA of *Lactococcus lactis* is an *N*-acetylglucosaminidase with an optimal number of LysM domains for proper functioning. *FEBS J* **272**: 2854-2868.

Steen, A., Buist, G., Leenhouts, K.J., El Khattabi, M., Grijpstra, F., Zomer, A.L., Venema, G., Kuipers, O.P., and Kok, J. (2003) Cell wall attachment of a widely distributed peptidoglycan binding domain is hindered by cell wall constituents. *J Biol Chem* **278**: 23874-23881.

Tiyanont, K., Doan, T., Lazarus, M.B., Fang, X., Rudner, D.Z., and Walker, S. (2006) Imaging peptidoglycan biosynthesis in *Bacillus subtilis* with fluorescent antibiotics. *Proc Natl Acad Sci USA* **103**: 11033-11038.

Vagner, V., Dervyn, E., and Ehrlich, D. (1998) A vector for systematic gene inactivation in *Bacillus subtilis*. *Microbiology* **144**: 3097-3104.

Varón, D., Boylan, S.A., Okamoto, K., and Price, C.W. (1993) *Bacillus subtilis gtaB* encodes UDP-glucose pyrophosphorylase and is controlled by stationary-phase transcription

factor σ^B. *J Bacteriol* **175**: 3964-3971.

Warth, A.D., and Strominger, J.L. (1971) Structure of the peptidoglycan from vegetative cell wall of *Bacillus subtilis*. *Biochemistry* **10**: 4349-4358.

Yamamoto, H., Kurosawa, S., and Sekiguchi, J. (2003) Localization of the vegetative cell wall hydrases LytC, LytE, and LytF on the *Bacillus subtilis* cell surface and stability of these enzymes to cell wall-bound or extracellular proteases. *J Bacteriol* **185**: 6666-6677.

Figure legends

Fig. 1. Localization of the LytF-, CWB_E- and CTD_E-6xFLAG fusion proteins.

A-C. Phase contrast (A) and LytF-6xFLAG localization (B) images, and an overlay image (C) of A and B (strain MH1022).

D-F. Phase contrast (D) and CWB_E-6xFLAG localization (E) images, and an overlay image (F) of D and E (strain YM1047).

G-I. Phase contrast (G) and CTD_E-6xFLAG localization (H) images, and an overlay image (I) of G and H (strain YM1051).

The OD_{600} value at the sampling time was 1.7 (late exponential phase). The exposure times were 0.1 s for phase contrast (A, D and G) and 0.1 s (gain 2) for Cy3 (B, E and H). In the case of panel H, the background of the image is raised in the image processing in order to detect weak signals. Scale bars, 10 μm.

Fig. 2. Western blot analysis of LytF-, CWB_E-, and CTD_E-6xFLAG fusions.

Cell surface proteins (lane C) and culture supernatant proteins (lane S) were prepared and subjected to Western blot analysis as described in Experimental procedures. The molecular masses of the protein standards (Bio-Rad) are indicated on the left. *B. subtilis* MH1022 (LytF-6xFLAG; 55 kDa), YM1047 (CWB_E-6xFLAG; 43 kDa), and YM1051 (CTD_E-6xFLAG; 19 kDa) were cultured in LB medium at 37˚C and were harvested at the late exponential phase (OD_{600}, 1.8). Proteins from the cell surface (lane C; equivalent to 5 OD_{600} cells per lane) and from the culture supernatant (lane S; equivalent to 5 OD_{600} cells per lane) were applied on a 12% polyacrylamide gel. Asterisks indicate the degradative products of LytF-6xFLAG.

Fig. 3. *In vitro* cell wall-binding assays with the GST-2xLysM protein.

In vitro cell wall-binding assays were examined in 60 µl of PBST buffer (80 mM NaH_2PO_4, 20 mM Na_2HPO_4, 100 mM NaCl [pH 7.5], and 1% Tween 20) containing 20 µg of the purified protein, and cell wall (CW) or peptidoglycan (PG) corresponding to 75 µg of PG. After 15-min incubation on ice, the reaction mixture was centrifuged to separate the supernatant, as the non-binding fraction, and the pellet, as the CW- or PG-binding fraction. Lane M, size marker (Bio Rad, each 1 µg); lane S, non-binding fraction; lane P, binding fraction. The ratios of the GST-2xLysM bands in lanes S and P calculated with a Lane and Spot Analyzer (ATTO) are shown under each lane.

A and B. CW- and PG-binding assays with GST-2xLysM (A) and GST-tECTD (B).

C. GST-2xLysM-binding assay to CWs prepared from TagB-depleted and TagO-depleted cells. *B. subtilis* HY1055 (P_{spac}-*tagB*) and MH1023 (P_{spac}-*tagO*) were first cultured in LB medium with 0.8 and 0.4 mM IPTG, respectively, at 37˚C to an OD_{600} of 0.5. Cells were harvested and inoculated at an OD_{600} of 0.03 into fresh LB medium with IPTG (0.8 mM, $TagB^+$; 0.4 mM, $TagO^+$) or without IPTG ($TagB^-$ and $TagO^-$). After incubation for 3 h, cells were harvested. CW amount in the binding assay was normalized in PG amount (75 µg in 60 µl of each reaction mixture) as described in Experimental procedures.

D. GST-2xLysM-binding assay to CW and PG prepared from a *tagO* null mutant strain. *B. subtilis* YM1052 (*tagO*::*kan*) was cultured in LB medium supplemented with 25 mM $MgCl_2$. Cells were grown to an OD_{600} of 1.6 and then harvested. CW and PG were prepared as described in Experimental procedures. Each reaction mixture (60 µl) included CW or PG corresponding to 75 µg of PG.

Fig. 4. Localization of LytF-6xFLAG in several WTA mutants.

Localization patterns of LytF-6xFLAG in *tagB* (A-G), *tagO* (H-O), *tagF* (P-U), and *ggaAB* (V and W) mutants were observed as follows. For culturing conditional mutants of *tagB* (HY1058; A-G), *tagO* (MH1031; H-M), and *tagF* (HY1059; P-U), the strains were first cultured in LB medium with the addition of IPTG (0.8 mM for HY1058, and 0.4 mM for MH1031 and HY1059) at 37˚C to an OD_{600} of 0.5. Cells were harvested and inoculated at an OD_{600} of 0.03 into fresh LB medium with or without IPTG. After incubation for 3 h, cells were harvested and fixed. Three sections at different levels in the z-axis after deconvolution were taken in a typical TagB-reduced cell (G).

N and O. Phase contrast (N) and LytF-6xFLAG localization (O) images of a *tagO* null mutant strain (HY1060). After the strain was cultured in LB medium with 25 mM $MgCl_2$ at 37˚C to an OD_{600} of 1.8, cells were harvested and fixed.

V and W. Phase contrast (V) and LytF-6xFLAG localization (W) images of a *ggaAB* double null mutant strain (MH1036). Cells were cultured in LB medium at 37˚C to an OD_{600} of 1.8. The exposure times were 0.1 s for phase-contrast images and 0.1 s (gain 2) for Cy3 images. Scale bars, 10 μm.

Fig. 5. Localization of LytF-6xFLAG in *mreBH*, *mbl* and *mreB* mutants.

A-D. Localization of LytF-6xFLAG in the wild-type (MH1022; A and B) and a *mreBH* null mutant (MH1042; C and D) strains. The strains were cultured in LB medium at 37˚C to an OD_{600} of 1.8.

E-N. Localization of LytF-6xFLAG in an *mbl*-conditional (HY1067; P_{xyl}-*mbl*) (E-H) and a *mreB*-conditional (HY1071; P_{xyl}-*mreB*) (I-N) mutant strains. The strains were first cultured in LB medium with xylose (12 mM for HY1067 and 2 mM for HY1071) at 37˚C to an OD_{600}

of 0.5. Cells were harvested and inoculated at an OD_{600} of 0.03 into fresh LB medium with or without xylose. When cells reached to an OD_{600} of 1.8, cells were harvested and fixed.

O-T. Localization of LytF-6xFLAG in a *mreB* null mutant strain (HY1075) grown with 25 mM (O and P), 2.5 mM (Q and R), and without (S and T) $MgCl_2$. The strain was first cultured in LB medium supplemented with 25 mM $MgCl_2$ at 37˚C to an OD_{600} of 0.5. Cells were harvested and inoculated at an OD_{600} of 0.03 into fresh LB medium with or without $MgCl_2$. After incubation for 3 h, cells were harvested and fixed.

The exposure times were 0.1 s for phase-contrast images and 0.1 s (gain 2) for Cy3 images. Scale bars, 10 μm.

Table 1. Bacterial strains and plasmids used in this study.

Strain and plasmid	Relevant genotype	Source[b] or Reference
Bacillus subtilis		
168	*trpC2*	S. D. Ehrlich
MH1018	*trpC2* Δ*wprA*	pMADWPRA→168
MH1019	*trpC2* Δ*epr* Δ*wprA*	pMADEPR→MH1018
MH1020	*trpC2 lytF*::pCA6FLCE (*lytF-6xflag cat*)	pCA6FLCE→168
YM1046	*trpC2 lytF*::pCA6FLCWB$_E$ (*cwb$_E$-6xflag cat*) (without the C-terminal catalytic domain of LytF)	pCA6FLCWB$_E$→168
YM1048	*trpC2* Ω(*lytF*::*ctd$_E$-6xflag cat*) (without the N-terminal 5xLysM domain of LytF)	Supplementary material
MH1022	*trpC2* Δ*epr* Δ*wprA lytF*::pCA6FLCE (*lytF-6xflag cat*)	MH1020→MH1019
YM1047	*trpC2* Δ*epr* Δ*wprA lytF*::pCA6FLCWB$_E$ (*cwb$_E$-6xflag cat*)	YM1046→MH1019
YM1051	*trpC2* Δ*epr* Δ*wprA* Ω(*lytF*::*ctd$_E$-6xflag cat*)	YM1048→MH1019
MH1024	*trpC2* Ω(*ggaAB*::*spc*)	pBGABSp→168
HY1053	*trpC2 pbpB'*::*lacZ lacI bla ermC* P$_{spac}$-*pbpB*	pM4PBPB2→168
HY1055	*trpC2 tagB'*::*lacZ lacI bla ermC* P$_{spac}$-*tagB*	pM4TAGB→168
HY1056	*trpC2 tagF'*::*lacZ lacI bla ermC* P$_{spac}$-*tagF*	pM4TAGF→168
MH1023	*trpC2 tagO'*::*lacZ lacI bla ermC* P$_{spac}$-*tagO*	pM4TAGO→168
YM1052	*trpC2* Ω(*tagO*::*kan*)	pGtagOKm→168
MH1029	*trpC2* Ω(*thrC*::P$_{xyl}$-*mreB spc*)	pXTMreB→168
HY1064	*trpC2* Ω(*thrC*::P$_{xyl}$-*mbl spc*)	pXTMbl→168
HY1065	*trpC2* Ω(*thrC*::P$_{xyl}$-*mbl spc*) Ω(*mbl*::*kan*)	pBmblKm96→ HY1064
MH1027	*trpC2* Ω(*mreBH*::*kan*)	pBmBH2941→168
HY1054	*trpC2* Δ*epr* Δ*wprA lytF*::pCA6FLCE (*lytF-6xflag cat*) *pbpB'*::*lacZ lacI bla ermC* P$_{spac}$-*pbpB*	HY1053→MH1022
HY1058	*trpC2* Δ*epr* Δ*wprA lytF*::pCA6FLCE (*lytF-6xflag cat*) *tagB'*::*lacZ lacI bla ermC* P$_{spac}$-*tagB*	HY1055→MH1022
HY1059	*trpC2* Δ*epr* Δ*wprA lytF*::pCA6FLCE (*lytF-6xflag cat*) *tagF'*::*lacZ lacI bla ermC* P$_{spac}$-*tagF*	HY1056→MH1022
MH1031	*trpC2* Δ*epr* Δ*wprA lytF*::pCA6FLCE (*lytF-6xflag cat*) *tagO'*::*lacZ lacI bla ermC* P$_{spac}$-*tagO*	MH1023→MH1022
HY1060	*trpC2* Δ*epr* Δ*wprA lytF*::pCA6FLCE (*lytF-6xflag cat*) Ω(*tagO*::*kan*)	YM1052→MH1022
MH1036	*trpC2* Δ*epr* Δ*wprA lytF*::pCA6FLCE (*lytF-6xflag cat*) Ω(*ggaAB*::*spc*)	MH1024→MH1022
MH1042	*trpC2* Δ*epr* Δ*wprA lytF*::pCA6FLCE (*lytF-6xflag cat*) Ω(*mreBH*::*kan*)	MH1027→MH1022
HY1066	*trpC2* Δ*epr* Δ*wprA lytF*::pCA6FLCE (*lytF-6xflag cat*) Ω(*thrC*::P$_{xyl}$-*mbl spc*)	HY1064→MH1022
HY1067	*trpC2* Δ*epr* Δ*wprA lytF*::pCA6FLCE (*lytF-6xflag cat*) Ω(*thrC*::P$_{xyl}$-*mbl spc*) Ω(*mbl*::*kan*)	HY1065→HY1066
HY1069	*trpC2* Δ*epr* Δ*wprA* Ω(*thrC*::P$_{xyl}$-*mreB spc*)	HY1064→MH1019
HY1070	*trpC2* Δ*epr* Δ*wprA* Ω(*thrC*::P$_{xyl}$-*mreB spc*) Δ*mreB*	pMADmreB→HY1069

HY1071	*trpC2* Δ*epr* Δ*wprA* Ω(*thrC*::P_{xyl}-*mreB spc*) Δ*mreB lytF*::pCA6FLCE (*lytF-6xflag cat*)	MH1020→HY1070
HY1072	*trpC2* Ω*kan* (*kan* is inserted between stop codon and terminator downstream of *minD*)	pBminDKm→168
HY1073	*trpC2* Δ*mreB* Ω*kan*	pMADmreB→HY1072
HY1075	*trpC2* Δ*epr* Δ*wprA lytF*::pCA6FLCE (*lytF-6xflag cat*) Δ*mreB* Ω*kan*	HY1073→MH1022
Escherichia coli		
JM109	*recA1 supE44 endA1 hsdR17 gyrA96 relA1 thi-1* Δ(*lac-proAB*) /F' [*traD36 proAB*$^+$ *lacI*^{q} *lacZ*ΔM15]	TaKaRa
C600	*supE44 hsdR17 thi-1 thr-1 leuB6 lacY1 tonA21*	Laboratory stock
BL21	F$^-$ *ompT hsdS*$_B$ (r_B^- m_B^-) *gal dcm'*	TaKaRa
Plasmids		
pBluescriptII SK+	*bla*	TOYOBO
pBGABSp	*bla* Δ*ggaAB*::*spc*	This study
pBmreBHfb	*bla* Δ*mreBH*	This study
pBmBH2961	*bla* Δ*mreBH*::*kan*	This study
pBmblfb	*bla* Δ*mbl*	This study
pBmblKm	*bla* Δ*mbl*::*kan*	This study
pBminDKm	*bla kan* (*kan* is inserted between stop codon and terminator downstream of *minD*)	This study
pCA3xFLAG	*bla cat 3xflag*	Yamamoto *et al*. (2003)
pCA3FLCE	*bla cat lytF-3xflag*	Yamamoto *et al*. (2003)
pCA6xFLAG	*bla cat 6xflag*	This study
pCA6FLCE	*bla cat lytF-6xflag*	This study
pCA6FLCWB$_E$	*bla cat cwb$_E$* (cell wall binding domain of LytF)-*6xflag*	This study
pDG1727	*bla spc*	BGSC [a]
pDG646	*bla ermC*	BGSC [a]
pDG782	*bla kan*	BGSC [a]
pDG783	*bla kan*	BGSC [a]
pGEX-2T	*bla gst*	GE Healthcare
pGEX-2xLysM	*bla gst-2xlysM*	This study
pGEM-3Zf(+)	*bla lacZ*	Promega
pGtagOKm	*bla* Δ*tagO*::*kan*	This study
pQECEtCTD	*bla 6xhis-ctd$_E$* (catalytic domain of LytF)	Ohnishi *et al*. (1999)
pGEXEtCTD	*bla gst- ctd$_E$* (catalytic domain of LytF)	This study
pMAD	*bla ermC bgaB*	Arnaud *et al*. (2004)
pMADWPRA	*bla ermC bgaB* Δ*wprA*	This study
pMADEPR	*bla ermC bgaB* Δ*epr*	This study
pMADmreB	*bla ermC bgaB* Δ*mreB*	This study
pMUTIN4	*lacZ lacI bla ermC*	Vagner *et al*. (1998)
pM4PBPB2	pMUTIN4::Δ*pbpB* (containing *pbpB* Shine-Dalgarno sequence)	This study
pM4TAGB	pMUTIN4::Δ*tagB* (containing *tagB* Shine-Dalgarno sequence)	This study
pM4TAGF	pMUTIN4::Δ*tagF* (containing *tagF* Shine-Dalgarno sequence)	This study

pM4TAGO	pMUTIN4::Δ*tagO* (containing *tagO* Shine-Dalgarno sequence)	This study
pXT	*bla thrC*::(P_{xyl} *spc*) *ermC*	Derré *et al*. (2000)
pXTMbl	*bla thrC*::(P_{xyl}-*mbl spc*) *ermC*	This study
pXTMreB	*bla thrC*::(P_{xyl}-*mreB spc*) *ermC*	This study

a : BGSC, *Bacillus* Genetic Stock Center, Ohio State University.

b: Sources shown before and after the arrows indicate donor DNA and recipient cells on transformation, respectively.

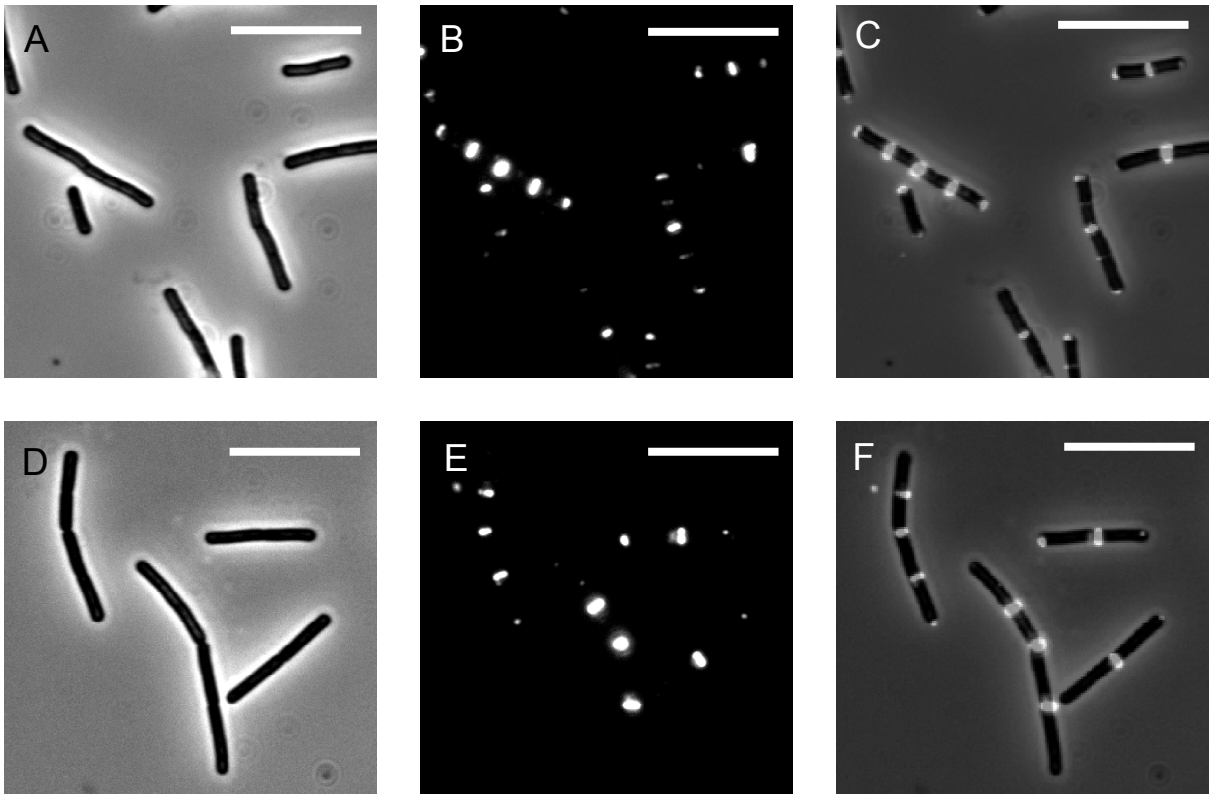

Fig. 1 Yamamoto *et al*.

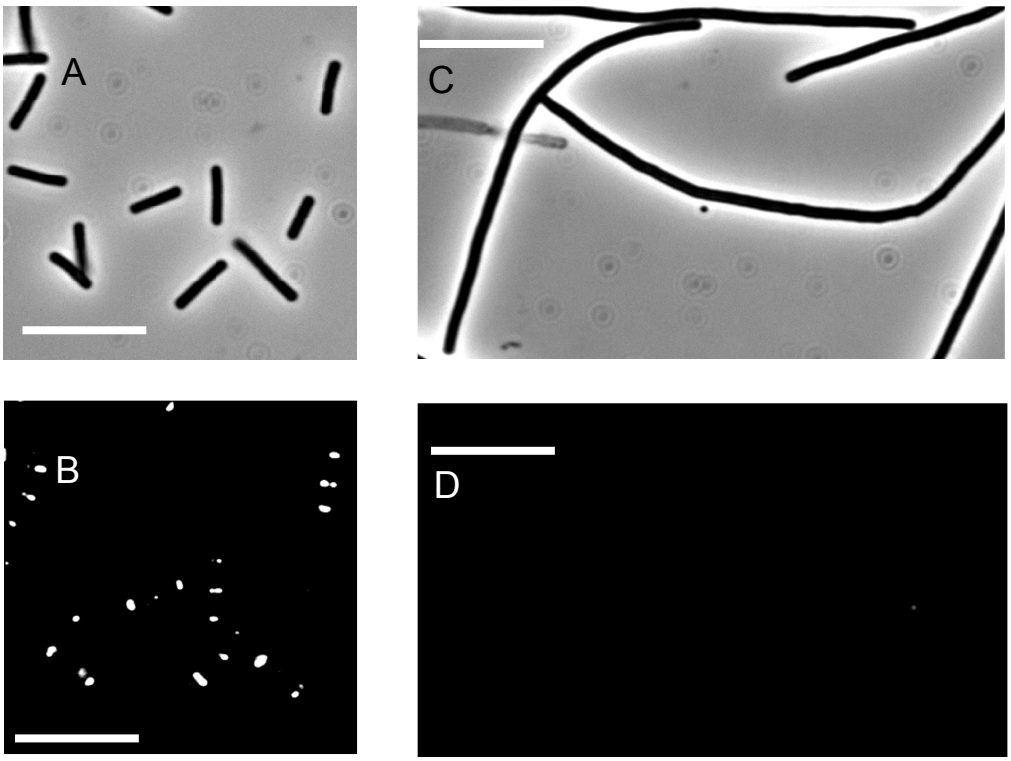

Fig. 2 Yamamoto *et al.*

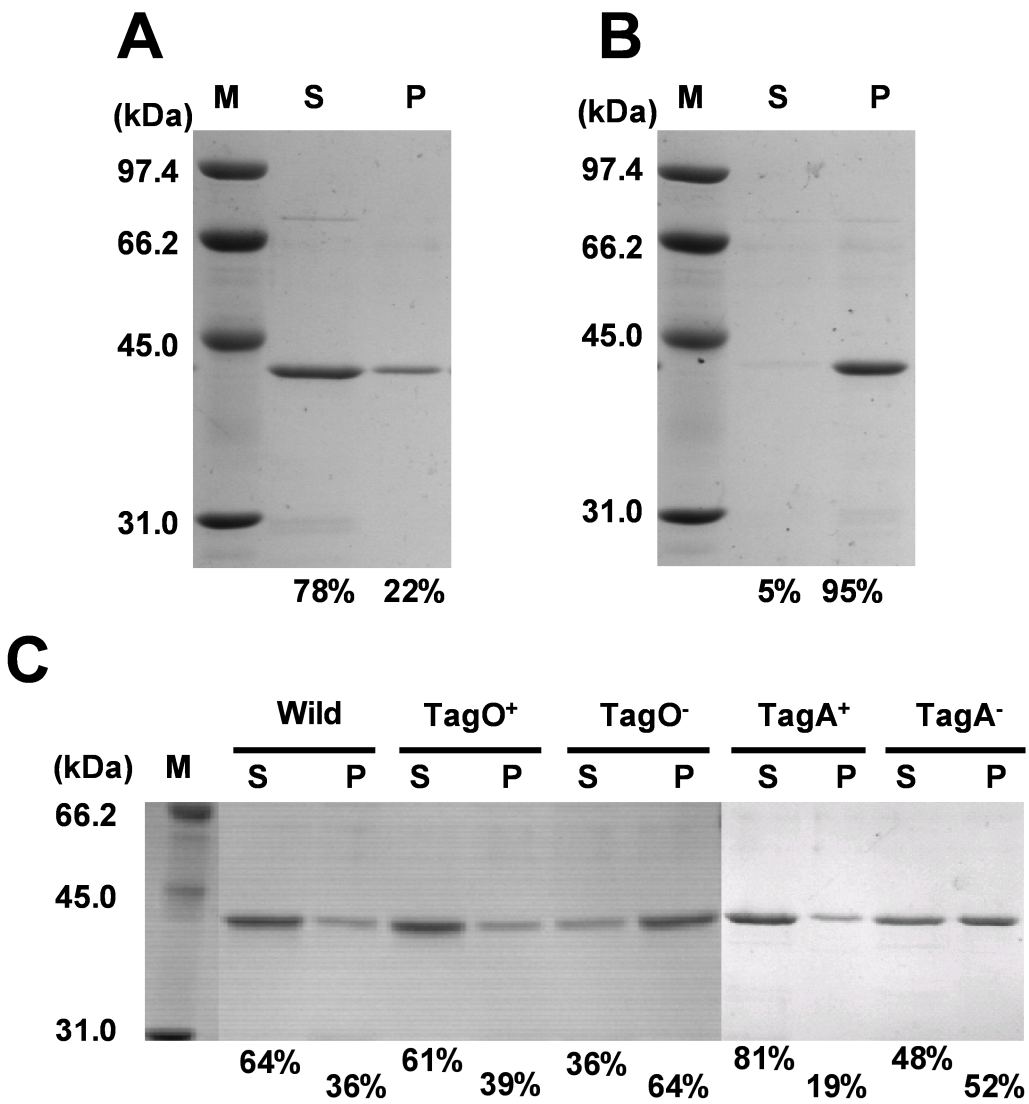

Fig. 3 Yamamoto *et al*.

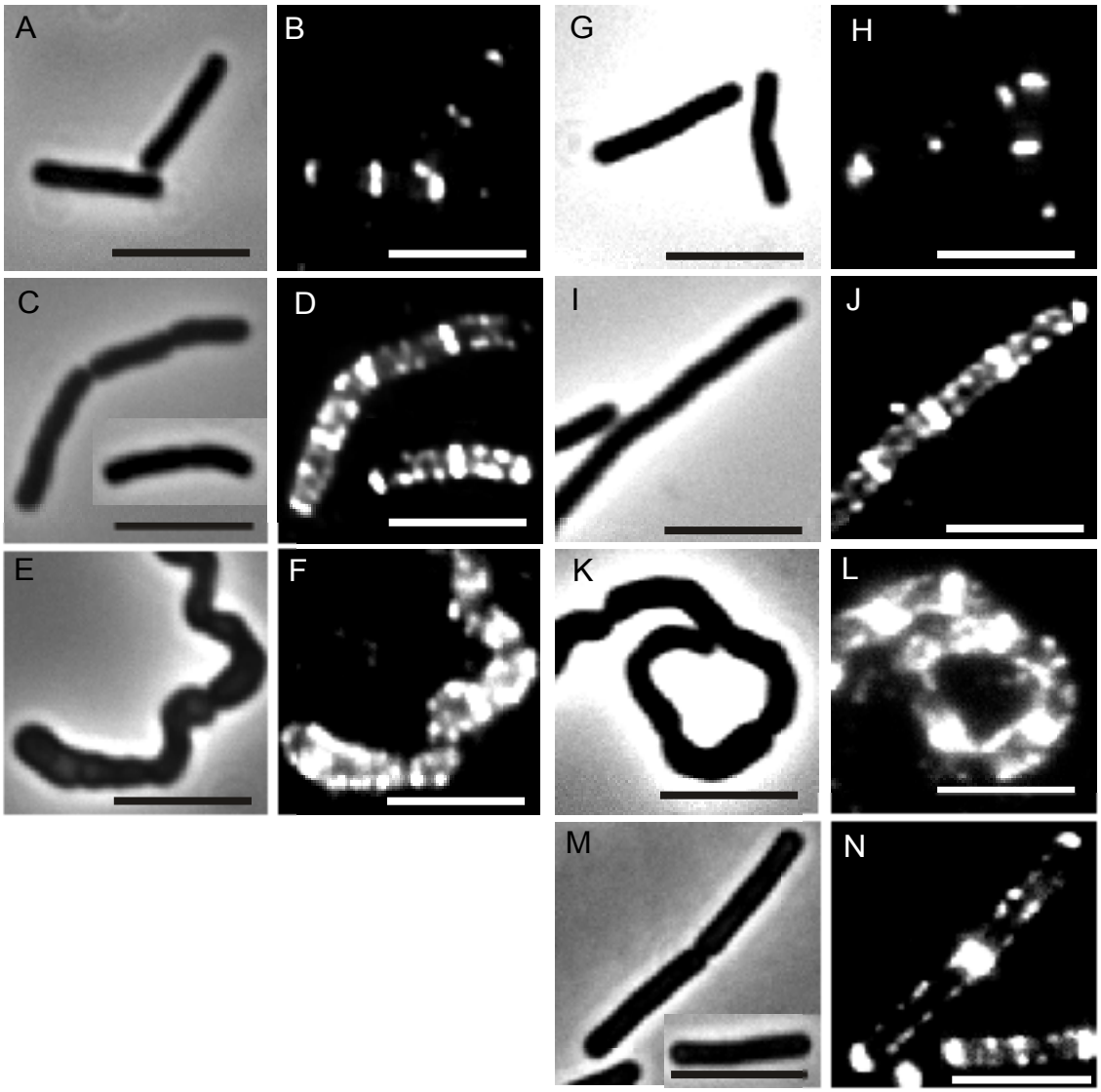

Fig. 4 . Yamamoto *et al.*

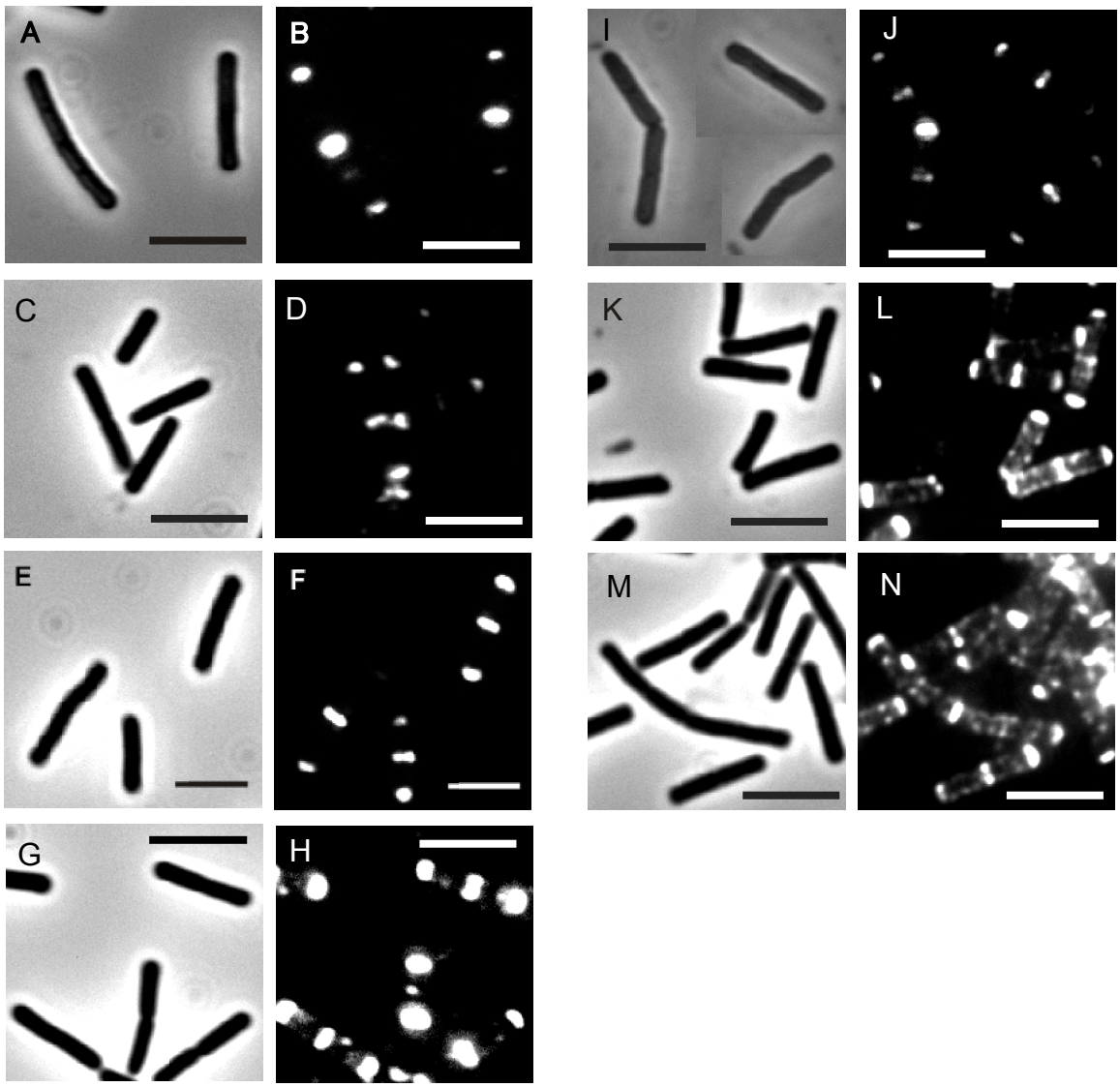

Fig. 5 Yamamoto *et al.*

Supporting Movie S1 legend

Movie S1. A z-stack image of LytF-6xFLAG in a TagB-reduced cell.

Localization patterns of LytF-6xFLAG in *tagB*-reduced cells were observed as follows. For culturing a *tagB*-conditional mutant (HY1058), the strain was first cultured in LB medium with the addition of 0.8 mM IPTG at 37˚C to an OD_{600} of 0.5. Cells were harvested and incubated at an OD_{600} of 0.03 into fresh LB medium with 0.1 mM IPTG. After incubation for 3h, cells were harvested and fixed. A z-stack image was taken in a typical TagB-reduced cell. The exposure time was 0.1 s (gain 1) for Cy3 image.

Supporting Information

Experimental procedures

Plasmid construction

Primers used in this study are listed in *Supporting Information*, Table S1. After digestion with restriction enzymes, all DNA fragments were fractionated by 1% agarose gel electrophoresis and purified with QIAquick gel extraction kit (QIAGEN) according to the manufacturer's instructions.

To obtain pCA6xFLAG, a 434 bp DNA fragment containing multi cloning sites and the *3xflag* gene of pCA3xFLAG (Yamamoto *et al*., 2003) was amplified with primers FLAG-FX and FLAG-R, and pCA3xFLAG as a template. After digesting the fragment with *Eco*RI and *Stu*I, a 118 bp fragment containing the *3xflag* gene was purified and cloned into the *Eco*RI and *Sma*I sites of pCA3xFLAG to generate pCA6xFLAG. The resultant *6xflag* gene encoded a polypeptide consisting of 45 amino acids (DYKDHDGDYKDHDIDYKDDDEGADYKDHDGDYKDHDIDYKDDDDK, M_r=5,452).

To construct a LytF-6xFLAG fusion strain, the 3' region of the *lytF* gene was obtained from pCA3FLCE (Yamamoto *et al*., 2003) digested with *Hin*dIII and *Bam*HI. The fragment was subcloned into the corresponding sites of pCA6xFLAG to generate pCA6FLCE.

To construct a gene fusion between the CW-binding domain of LytF (CWB_E) and the 6xFLAG epitope-tag, the internal region of *lytF* (*cwlE*; 361 bp) just before the catalytic domain was amplified by PCR using the *B. subtilis* 168 chromosomal DNA (168

chrDNA) as a template, and primers CWBE-Ef and CWLE-GRX. After the amplified fragment had been digested with *Eco*RI and *Xba*I, the digested fragments were ligated into the corresponding sites of pCA6xFLAG to generate pCA6FLCWB_E. After sequencing, the plasmids were used for transformation of *E. coli* C600 to produce concatemeric plasmid DNAs.

To construct a *pbpB*-conditional mutant, the 5'-terminal region including the ribosome-binding site was amplified by PCR using 168 chrDNA as the template, and primers pB-HFSD2 and PBPB-BR. The amplified 244-bp fragment was digested with *Hin*dIII and *Bam*HI, and then the resultant fragment was cloned into the corresponding sites of pMUTIN4 (Vagner *et al*., 1998) to obtain pM4PBPB2. For construction of *tagB*-, *tagO*-, and *tagF*-conditional mutants, the 5'-terminal regions including the ribosome binding sites were amplified by PCR using 168 chrDNA as the template, and primers TAGBp-Ef and TAGBp-Br for *tagB* (397 bp), TagOSD-EF and TagOSD-BR2 for *tagO* (300 bp), and TAGFp-Ef and TAGFp-Br for *tagF* (393 bp), respectively. The amplified fragments were digested with *Eco*RI and *Bam*HI, and then ligated into the corresponding sites of pMUTIN4 to obtain pM4TAGB, pM4TAGO, and pM4TAGF. After sequencing, the plasmids were used for transformation of *E. coli* C600 to generate concatemeric DNAs.

For construction of a *ggaA* and *ggaB* double mutant, an upstream fragment of *ggaA* (656 bp) and a downstream one of *ggaB* (603 bp) were amplified with 168 chrDNA as the template, and primers ggaAF-Bf and ggaAF-Er for *ggaA*, and primers ggaBB-Spf and ggaBB-Kr for *ggaB*, respectively. The amplified fragments were digested with *Eco*RI for *ggaA* and *Sph*I for *ggaB*, and then the digested fragments were ligated with an *Eco*RI-*Sph*I digested fragment carrying a spectinomycin resistance cassette derived

from pDG1727. The ligation mixture was used as a template for second PCR with primers ggaAF-Bf and ggaBB-Kr. The resultant PCR fragment (2.4 kb) was digested with *Bam*HI and *Kpn*I, and then ligated into appropriate sites of pBluescriptII SK+ to generate pBGABSp.

To construct a double mutant for *epr* and *wprA* without any antibiotic resistance cassette, we used an efficient allelic replacement method with pMAD (Arnaud *et al*., 2004). Upstream (504 bp) and downstream (510 bp) regions of the *epr* gene were amplified with two sets of primers, eprf-Bf and eprf-Kr, and eprb-Kf and eprb-Nr, respectively, and 168 chrDNA as a template. The amplified fragments were digested with *Kpn*I. Then the fragments were ligated and the ligation mixture used as a template for 2nd PCR with eprf-Bf and eprb-Nr. After digestion with *Bam*HI and *Nco*I, the resulting 1.0-kb DNA fragment was cloned into the corresponding sites in pMAD to obtain pMADEPR. A similar procedure was used to construct pMADWPRA. The two sets of primers used for 1st PCR amplification for the upstream (495 bp) and downstream (498 bp) fragments were wprAf-Bf and wprAf-Kr, and wprAb-Kf and wprAb-Nr, respectively.

To construct a *mreBH* null mutant, upstream (474 bp) and downstream (463 bp) regions of *mreBH* were amplified with two sets of primers, mreBHf-Kf and mreBHf2Ebr, and mreBHb2Ef and mreBHb-Sr, respectively, and 168 chrDNA as a template. The amplified fragments were digested with *Eco*RI. Then the fragments were ligated and the ligation mixture was used as a template for 2nd PCR with mreBHf-Kf and mreBHb-Sr. After digestion with *Kpn*I and *Sal*I, the resulting 0.94-kb DNA fragment was cloned into the corresponding sites in pBluescriptII SK+ to obtain pBmreBHfb. A *Bgl*II-*Eco*RI-digested kanamycin resistance gene cassette derived from

pDG782 was ligated into the *Bam*HI and *Eco*RI sites of pBmreBHfb to generate pBmBH2961.

To construct xylose-inducible *mbl* and *mreB* genes, the intact *mbl* and *mreB* genes with the SD sequences were amplified with primers MBL-BF and MBL-ER for *mbl* (1020 bp), and MreBSD-Bf and MreBSD-Er for *mreB* (1037 bp), respectively, and 168 chrDNA as a template. After double digestion with *Bam*HI and *Eco*RI, the resultant fragments were cloned into the corresponding sites in pXT (Derré *et al*., 2000) to generate pXTMbl and pXTMreB.

To obtain the plasmid used for the construction of an *mbl*-conditional mutant, upstream (602 bp) and downstream (606 bp) fragments of the *mbl* gene were amplified by PCR with 168 chrDNA as a template, and two pairs of primers, mblF-Hf and mblF-Er, and mblB-EBf and mblB-Xr, respectively. After digesting with *Eco*RI, the fragments were ligated. The ligation mixture was used as a template for 2nd PCR with primers mblF-Hf and mblB-Xr. The amplified fragment was digested with *Hin*dIII and *Xba*I, then cloned into the corresponding sites of pBluescriptII SK+ to generate pBmblfb. Next, a kanamycin resistance gene of pDG782 was digested with *Eco*RI and *Bgl*II, and the fragment was cloned into *Eco*RI and *Bam*HI sites of pBmblfb to obtain pBmblKm.

To obtain the plasmid used for the construction of an in-frame *mreB* mutant, upstream (521 bp) and downstream (513 bp) fragments of the *mreB* gene were amplified by PCR with 168 chrDNA as a template, and two pairs of primers, mreBf-1Bf and mreBf-2r, and mreBb-3f and mreBb-4Nr, respectively. These two DNA fragments were mixed and used as a template of 2nd PCR with primers mreBf-1Bf and mreBb-4Nr. The resultant amplified fragment (1034 bp) was digested with *Bam*HI and *Nco*I. After digestion, the

fragment was cloned into the corresponding sites in pMAD to obtain pMADmreB.

To obtain a plasmid used for the construction of a *tagO* null mutant, upstream (640 bp) and downstream (648 bp) fragments of the *tagO* gene were amplified by PCR with 168 chrDNA as a template, and two pairs of primers, tagOf-Sf and tagOf-Pr, and tagOb-Bgf and tagOb-Xr, respectively. Then the fragments were digested with *Pst*I and *Bgl*II, respectively. Moreover, a kanamycin resistance gene of pDG783 was digested with *Pst*I and *Bam*HI. After ligation with these three fragments, the ligation mixture was used as a template for 2nd PCR with primers tagOf-Sf and tagOb-Xr. After the amplified DNA fragment was digested with *Sac*I and *Xba*I, the fragment was cloned into the corresponding sites of pGEM-3Zf(+) to produce pGtagOKm.

For construction of a kanamycin resistance marker inserted downstream of the *minD* gene, upstream (540 bp) and downstream (507 bp) fragments of the stop codon of the *minD* gene were amplified by PCR with 168 chrDNA as a template, and two pairs of primers, minDf-Xf and minDf-BEr, and minDb-Ef and minDb-Mr, respectively. Then the fragments were digested with *Bam*HI and *Eco*RI, respectively. Moreover, the promoter- and terminator-less kanamycin resistance gene was amplified by PCR with primers Km-Bgf and Km-Er, and pDG782 as a template. The amplified kanamycin resistance cassette (827 bp) was digested with *Bgl*II and *Eco*RI. After ligation with these three fragments, the ligation mixture was used as a template for 2nd PCR with primers minDf-Xf and minDb-Mr. After the amplified DNA fragment (1.87 kb) was digested with *Xba*I and *Mun*I, the fragment was cloned into the *Xba*I and *Eco*RI sites of pBluescriptII SK+ to produce pBminDKm.

For construction of a glutathione S-transferase (GST)-2xLysM expression plasmid, an internal fragment (448 bp) of *lytF* was amplified with 168 chrDNA as the template,

and primers CwlE-BF and CWBE-KR2. The fragment was digested with *Bam*HI and *Kpn*I, and then ligated into the corresponding sites of pGEX-2T to generate pGEX-2xLysM. For construction of GST fused by the C-terminal catalytic domain of LytF (GST-EtCTD), pQECEtCTD (Ohnishi *et al*., 1999) was digested with *Bam*HI and *Sma*I. The resultant fragment (450 bp) was subcloned into the corresponding sites of pGEX-2T, to generate pGEXEtCTD. The nucleotide sequences of all inserts amplified by PCR were confirmed by sequencing.

Construction of mutants and FLAG fusion strains

The sources of donor DNAs and recipient cells used for *B. subtilis* mutant construction are listed in Table 1. To construct a *wprA* and *epr* double null mutant, *B. subtilis* MH1019, without any antibiotic resistance genes, we used an efficient allelic replacement method with the pMAD plasmid (Arnaud *et al*., 2004). First, to construct a *wprA* null mutant, *B. subtilis* 168 was transformed with pMADWPRA. A blue colony was selected on a LB plate containing 0.3 μg ml^{-1} of erythromycin and 200 μg ml^{-1} of X-gal (5-bromo-4-chloro-3-indolyl-β-D-galactopyranoside). We performed the subsequent integration and excision procedures as described by Arnaud *et al*. (2004). After the excision procedure, we selected some white and erythromycin-sensitive colonies to obtain *B. subtilis* MH1018. Finally, we confirmed the proper null mutation at the *wprA* locus by PCR with primers WPRA-UP and WPRA-DN. Next, *B. subtilis* MH1018 was transformed with pMADEPR to obtain a *wprA* and *epr* double null mutant, *B. subtilis* MH1019. After integration and excision procedures, we checked the proper null mutation at the *epr* locus by PCR with primers EPR-UP and EPR-DN.

For construction of a *ggaA* and *ggaB* double mutant strain, pBGABSp linearized with *Aat*II was used for transformation of *B. subtilis* 168 to obtain *B. subtilis* MH1024. To construct a *tagO* null mutant, *B. subtilis* 168 was transformed with pGtagOKm linearlized with *Sph*I to obtain YM1052. For construction of *pbpB*-, *tagB*-, *tagF*- and *tagO*-conditional mutants, *B. subtilis* 168 was transformed with pM4PBPB2, pM4TAGB, pM4TAGF and pM4TAGO to obtain *B. subtilis* HY1053, HY1055, HY1056 and MH1023, respectively. The resultant transformants were selected on LB agar plates containing erythromycin and IPTG.

To construct *B. subtilis* MH1020, which has a LytF-6xFLAG fusion at the *lytF* locus, pCA6FLCE was used for transformation of *B. subtilis* 168. The mature LytF-6xFLAG fusion protein (513 amino acids; M_r, 54,848) appears to consist of full length 462 amino acids of LytF without the signal peptide, followed by a short linker sequence (six amino acids; ARGSRA) and the 6xFLAG epitope-tag sequence.

To construct *B. subtilis* YM1046, which has a CWB_E-6xFLAG fusion at the *lytF* locus, pCA6FLCWB_E was used for transformation of *B. subtilis* 168. The mature CWB_E-6xFLAG fusion protein (401 amino acids; M_r, 42,608) appears to consist of the N-terminal 350 amino acids of LytF without the signal peptide, followed by a short linker sequence (six amino acids; SRGSRA) and the 6xFLAG epitope-tag sequence.

For construction of the C-terminal catalytic domain (CTD) fused by 6xFLAG, an upstream DNA fragment (900 bp) including the signal sequence of the *lytF* gene, and a downstream DNA fragment (906 bp) were amplified with primers LF1-NTDf and LF2-NTDr, and Cm5-LFCTDf and LF6-CTDr, respectively, and 168 chrDNA as a template. In addition, a DNA fragment (1,641 bp) including the *ctd_E-6xflag* and the following *cat* gene was amplified with primers, LF3-CTDf and Cm4-CTDr, and the

chromosomal DNA of MH1020 as a template. These three DNA fragments were mixed and used as a template of 2nd PCR with primers LF1-NTDf and LF6-CTDr. The resultant 3.45-kb amplified fragment was used for the *B. subtilis* transformation to obtain a strain YM1048. The strain would produce a truncated LytF-6xFLAG fusion protein lacking the N-terminal LysM domain. The mature CTD_E-6xFLAG fusion protein (172 amino acids; M_r, 19,223) appears to consist of the C-terminal 121 amino acids of LytF followed by a short linker sequence (six amino acids; ARGSRA) and the 6xFLAG epitope-tag sequence. The gene order around the *lytF* locus of the strain is *yhdE*, P_{lytF}, the signal peptide of *lytF*, the C-terminal catalytic domain of *lytF*, *6xflag*, *cat*, and *yhdC*.

To construct a *mreBH* null mutant, *B subtilis* 168 was transformed with pBmBH2961 linearized with *Sca*I to obtain MH1027. To construct a xylose-inducible *mbl* conditional mutant, firstly, a xylose-inducible ectopic copy (P_{xyl}-*mbl*) was constructed on the *thrC* locus. For this purpose, *B subtilis* 168 was transformed with pXTMbl linearized with *Aat*II to obtain HY1064. Next, to introduce an *mbl* null mutation (*mbl*::*kan*) at the *mbl* locus, *B subtilis* HY1064 was transformed with pBmblKm linearlized with *Sca*I to obtain HY1065. All strains were confirmed by PCR.

To construct a xylose-inducible *mreB* conditional mutant, *B subtilis* MH1019 was transformed with pXTMreB linearized with *Aat*II to obtain HY1069. As a result, a xylose-inducible ectopic copy (P_{xyl}-*mreB*) was constructed on the *thrC* locus. Next, to introduce an in-frame *mreB* mutation, pMADmreB was transformed into HY1069. To obtain HY1070, then we performed the subsequent integration and excision procedures as described by Arnaud *et al*. (2004). After checking by PCR, we confirmed the in-frame mutation at the *mreB* locus by sequencing. The resultant strain HY1070 had an

in-frame deletion of *mreB* lacking all but the first and last 42 bases of the *mreB* coding region as described by Formstone and Errington (2005).

To introduce a kanamycin resistance marker downstream of the *minD* gene, *B subtilis* 168 was transformed with pBminDKm linearized with *Kpn*I. In the resultant strain HY1072, the *kan* gene was inserted between the stop codon and the terminator downstream of the *minD* gene. We confirmed that this *kan* marker insertion does not affect cell morphology and growth.

References

Arnaud, M., Chastanet, A., and Débarbouillé, M. (2004) New vector for efficient allelic replacement in naturally nontransformable, low-GC-content, Gram-positive bacteria. *Appl Environ Microbiol* **70**: 6887-6891.

Derré, I., Rapoport, G., and Msadek, T. (2000) The CtsR regulator of stress response is active as a dimmer and specifically degraded *in vivo* at 37˚C. *Mol Microbiol* **38**: 335-347.

Formstone, A., and Errington, J. (2005) A magnesium-dependent *mreB* null mutant: implications for the role of *mreB* in *Bacillus subtilis*. *Mol Microbiol* **55**: 1646-1657.

Ohnishi, R., Ishikawa, S., and Sekiguchi, J. (1999) Peptidoglycan hydrolase LytF plays a role in cell separation with LytE during vegetative growth of *Bacillus subtilis*. *J Bacteriol* **181**: 3178-3184.

Vagner, V., Dervyn, E., and Ehrlich, D. (1998) A vector for systematic gene inactivation in *Bacillus subtilis*. *Microbiology* **144**: 3097-3104.

Yamamoto, H., Kurosawa, S., and Sekiguchi, J. (2003) Localization of the vegetative

cell wall hydrases LytC, LytE, and LytF on the *Bacillus subtilis* cell surface and stability of these enzymes to cell wall-bound or extracellular proteases. *J Bacteriol* **185**: 6666-6677.

Supporting Table S1

Table S1. Primers used in this study.

Primer	Sequence(5'→3') [a]	Restriction site
CWBE-Ef	cgcgaattcTATAACCTGACTGTACAG	*Eco*RI
CWLE-GRX	gcgctctagaCATTGTGTTAATCTTCGCAC	*Xba*I
FLAG-FX	gccgctcgagTTGAGTGAGCTGATACCG	
FLAG-R	cggcaggcctCATCGTCATCCTTGTAGTC	*Stu*I
CwlE-BF	gccgggatccgatgacgatgacaaaGCAACGATTAAGGTCAAAA	*Bam*HI
CWBE-KR2	gccgggtacccgggtcaTGTTCCCGTAGAAGATGA	*Sma*I
pB-HFSD2	gcgcaagcttGGAGGAATGATTCAAATGCCA	*Hind*III
PBPB-BR	gcgcggatccTGTGTCCTCTGCAATGAC	*Bam*HI
TAGBp-Ef	gccgaattcAATGGATGATAAAAATGAAAATA	*Eco*RI
TAGBp-Br	ggcggatccTTTGCGTGCCATACTTGG	*Bam*HI
TagOSD-EF	cgcgaattcAAAGGAGACTTCTTTATGC	*Eco*RI
TagOSD-BR2	cgcggatccTCGTCAAGAATACCTAACAC	*Bam*HI
TAGFp-Ef	gccgaattcAAAGGAGGGTTAATGTCCTTAGTAG	*Eco*RI
TAGFp-Br	gccggatccAAGAGTGGTTCCTGCTC	*Bam*HI
MBL-BF	gcgcggatccAAGGAGGATATAAATAGATG	*Bam*HI
MBL-ER	cggcgaattcAGCTTAGTTTGCGTTTAG	*Eco*RI
ggaAF-Bf	cgcggatccCCTACCAATTCTACATTATC	*Bam*HI
ggaAF-Er	cgcgaattcGACACTCTCTATTGAATATC	*Eco*RI
ggaBB-Spf	cgcgcatgcCGTATGGAAGATAAGTATAG	*Sph*I
ggaBB-Kr	cgcggtaccGCTAAGTAAACACCACTTG	*Kpn*I
MreBSD-Bf	cgcggatccGAAAGGAAGATACATACATAT	*Bam*HI
MreBSD-Er	cgcgaattcCCGATTATCTAGTTTTCCC	*Eco*RI
mreBf-1Bf	gccggatccAACGAAGAACATTTCGT	*Bam*HI
mreBf-2r	TCCAAGATCTATACCAAGG	
mreBb-3f	CCTTGGTATAGATCTTGGAAAAGCACTGGAGCACATC	
mreBb-4Nr	gccgccatggCCATATCTTTCGCTAC	*Nco*I
minDf-Xf	gcgctctagaACGAGCGATAAGACAGC	*Xba*I
minDf-BEr	gccgaattcggatccTCACATTAAGATCTTACTCC	*Bam*HI
minDb-Ef	gcgcgaattcGAATCAAAGAGAAGAATCTG	*Eco*RI
minDb-Mr	gccaacaattgACCAATGGCTTGCTGAAG	*Mun*I
Km-Bgf	gcgcagatctACTGTAGAAAAGAGGAAGG	*Bgl*II
Km-Er	cggcgaattcGGTACTAAAACAATTCATCC	*Eco*RI
wprAf-Bf	gcgggatccCAGCTACTCGCTGTATTC	*Bam*HI
wprAf-Kr	cgcggtaccCGAGCTGAATTTTCTGCG	*Kpn*I
wprAb-Kf	cgcggtaccGAAGCAAAAGTTGTTGTTG	*Kpn*I
wprAb-Nr	cgcccatggCAACACAGCCCAATCTG	*Nco*I

WPRA-UP	gcgaagcttCCTACATATTACGACATGG	
WPRA-DN	gccgaattcATCGAAAACGGTGAAGGC	
eprf-Bf	cgcggatccCAAACGAAGCGTTAACAG	*Bam*HI
eprf-Kr	cgcggtaccGACTGATACAACAAGTTTG	*Kpn*I
eprb-Kf	cgcggtaccAAGCTGCAAAAACGGCTG	*Kpn*I
eprb-Nr	gcgccatggCCTGCGAGCAGCAGTAA	*Nco*I
EPR-UP	gcgaagcttACCATAGCTTTCTGCCAG	
EPR-DN	gccgaattcGTACAATGGCTGATGCTG	
mblF-Hf	gcgaagcttGTGGGCATATTTCACAAAC	*Hind*III
mblF-Er	cgcgaattcGAGGTCAATACCAATATCC	*Eco*RI
mblB-EBf	cgcgaattcggatccCCTAAACGCAAACTAAGCT	*Bam*HI
mblB-Xr	gcgtctagaCGTCAGCTGATTGTTCTC	*Xba*I
tagOf-Sf	cgcgagctcTGCAAAAGCCTGATTG	*Sac*I
tagOf-Pr	gcgctgcagCAACAATGCGAATCATGC	*Pst*I
tagOb-Bgf	gcgcagatctGTTTTATAAACGGCTGGTG	*Bgl*II
tagOb-Xr	gcgctctagaGCGAAGAAGCCTTAGCA	*Xba*I
LF1-NTDf	TTTATCCTTCGGCCTTGG	
LF2-NTDr	TGCTGCTTCAGCTGGTG	
LF3-CTDf	CACCAGCTGAAGCAGCAACGAGTGCGAAGATTAACA	
Cm4-CTDr	GTACAGTCGGCATTATCTC	
Cm5-LFCTDf	GAGATAATGCCGACTGTACCGGTGCAAAACGATATTTC	
LF6-CTDr	AGCATAAAAGAGCTTGTCG	
LF7-SEQf	ATACGATTATCGCACTTGC	
LF8-SEQr	ATATGAGAACTGTGATGCG	

[a]: The additional sequence (lowercase) and restriction site (under line) are indicated.

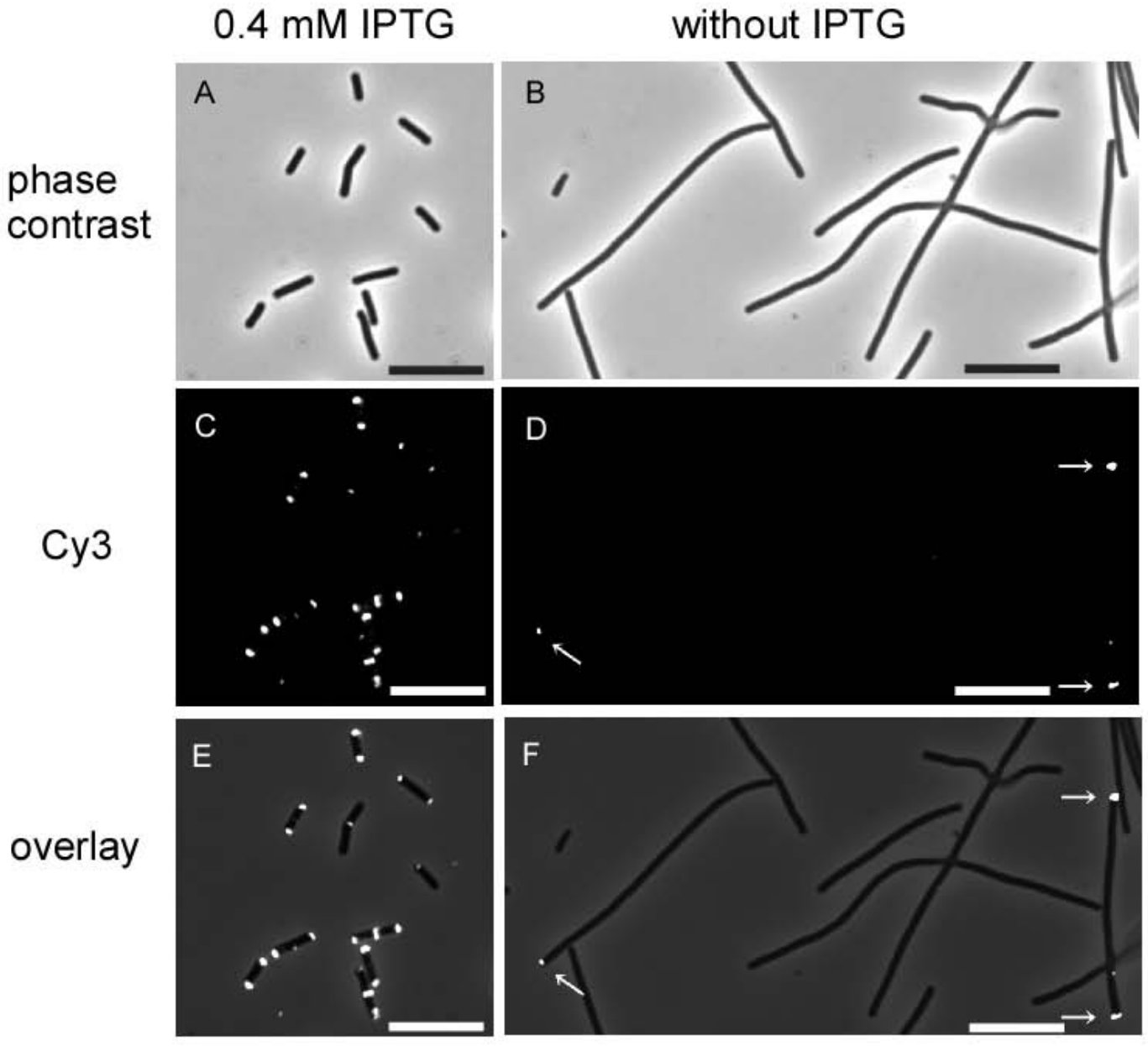

Fig. S1 . Yamamoto *et al.*

Supporting Figure S1 legend

Figure S1. LytF-6xFLAG localization in PBP 2B-depleted cells.

Phase contrast (A and B) and LytF-6xFLAG localization (C and D) images of a *pbpB*-conditional mutant strain (HY1054) with (A and C) and without (B and D) 0.4 mM IPTG. Overlay images of A and C, and of B and D are shown in panels E and F, respectively. The strain was first cultured in LB medium with 0.4 mM IPTG at 37˚C to an OD_{600} of 0.5. Cells were harvested and inoculated at an OD_{600} of 0.03 into fresh LB medium with or without IPTG. After incubation for 3 h, cells were harvested and fixed. The exposure times were 0.1 s for phase contrast (A and B) and 0.1 s (gain 2) for Cy3 (C and D). Arrows indicated positions of rare poles where LytF-6xFLAG foci appear to be observed in PBP 2B-depleted filaments. Scale bars, 10 μm.